



Contents lists available at ScienceDirect

Biochimie

journal homepage: www.elsevier.com/locate/biochi

Research paper

Treatment of rat thyrocytes *in vitro* with cathepsin B and L inhibitors results in disruption of primary cilia leading to redistribution of the trace amine associated receptor 1 to the endoplasmic reticulumJoanna Szumska^{a,1}, Zaina Batool^a, Alaa Al-Hashimi^{a,2}, Vaishnavi Venugopalan^{a,2}, Vladislav Skripnik^{a,2}, Norbert Schaschke^b, Matthew Bogyo^c, Klaudia Brix^{a,*}^a Department of Life Sciences and Chemistry, Jacobs University Bremen, Campus Ring 1, 28759 Bremen, Germany^b Fakultät für Chemie, Hochschule Aalen, 73430 Aalen, Germany^c Department of Pathology, Stanford University School of Medicine, Stanford, CA, USA

ARTICLE INFO

Article history:

Received 16 February 2019

Accepted 10 July 2019

Available online xxx

Keywords:

Activity based probes

Cysteine cathepsins

G-protein coupled receptor Taar1

Primary cilia

Thyroid epithelial cells

ABSTRACT

Taar1 is a G protein-coupled receptor (GPCR) confined to primary cilia of rodent thyroid epithelial cells. Taar1-deficient mouse thyroid follicles feature luminal accumulation of thyroglobulin suggesting that Taar1 acts as a regulator of extra- and pericellular thyroglobulin processing, which is mediated by cysteine cathepsin proteases present at the apical plasma membrane of rodent thyrocytes.

Here, by immunostaining and confocal laser scanning microscopy, we demonstrated co-localization of cathepsin L, but only little cathepsin B, with Taar1 at primary cilia of rat thyrocytes, the FRT cells. Because proteases were shown to affect half-lives of certain receptors, we determined the effect of cathepsin activity inhibition on sub-cellular localization of Taar1 in FRT cells, whereupon Taar1 localization altered such that it was retained in compartments of the secretory pathway. Since the same effect on Taar1 localization was observed in both cathepsin B and L inhibitor-treated cells, the interaction of cathepsin activities and sub-cellular localization of Taar1 was thought to be indirect. Indeed, we observed that cathepsin inhibition resulted in a lack of primary cilia from FRT cells. Next, we proved that primary cilia are a necessity for Taar1 trafficking to reach the plasma membrane of FRT cells, since the disruption of primary cilia by treatment with β -cyclodextrin resulted in Taar1 retention in compartments of the secretory pathway. Furthermore, in less well-polarized rat thyrocytes, namely in FRTL-5 cells lacking primary cilia, Taar1 was mainly confined to the compartments of the secretory pathway.

We conclude that Taar1 localization in polarized thyroid epithelial cells requires the presence of primary cilia, which is dependent on the proteolytic activity of cysteine cathepsins B and L.

© 2019 The Author(s). Published by Elsevier B.V. This is an open access article under the CC BY license (<http://creativecommons.org/licenses/by/4.0/>).

1. Introduction

Recently, we found the Trace amine-associated receptor 1 (Taar1), a G protein coupled receptor (GPCR), to be localized at primary cilia of rat thyrocytes, namely, FRT cells *in vitro*, and at antennae-like projections abundant at the apical plasma membrane domain of mouse thyrocytes *in situ* [1]. The apical plasma

membrane of thyroid epithelial cells faces the extracellular follicle lumen, which is a location where processes occur that are essential for thyroid function. First, iodination of thyroglobulin (Tg) by thyroid peroxidase (TPO) takes place in the direct vicinity of the apical plasma membrane before Tg is stored in the follicle lumen [2,3]. Second, the initial steps of Tg processing for thyroid hormone (TH) liberation happen at the apical plasma membrane and are mediated by cysteine cathepsins secreted into the follicle lumen upon thyroid stimulating hormone (TSH)-stimulation of thyrocytes [4–7]. The protein amounts and activities of Tg-processing cathepsins B and L in mouse thyrocytes were affected by Taar1-mediated signalling as was shown in a Taar1-deficient mouse model [8]. Interestingly, one of the Tg-processing proteases, cathepsin L, was found to be associated with primary cilia of well-polarized porcine thyrocytes upon

* Corresponding author.

E-mail address: k.brix@jacobs-university.de (K. Brix).

¹ Present address of JS is Department of Internal Medicine III, Cardiology, Angiology and Respiratory Medicine, Universitätsklinikum Heidelberg, Im Neuenheimer Feld 669, D-69120 Heidelberg, Germany.

² These authors contributed equally to this work.

short-term culture of cells isolated from thyroid tissue [9]. These findings indicated the presence of both, cathepsin L and Taar1, at cilia of differentiated thyrocytes *in situ* in physiological thyroid states. Because Taar1 deficiency in mice also affected TSH regulation of the thyroid gland in that TSH receptors were non-canonically localized to intracellular compartments [8], the question arose whether TSH-dependent secretion of cysteine cathepsins, their association with the apical plasma membrane, their inhibition by cystatins and thyroglobulin-derived thyropins, or all of these, depend on Taar1 localized to primary cilia. Therefore, in this study we asked how inhibition of the thyroglobulin-processing cysteine cathepsins affects Taar1 localization at primary cilia of thyrocytes.

Functionally significant interactions of certain GPCRs, e.g. protease activated receptors (PARs) 1–4, and proteases e.g. thrombin, at the plasma membrane of epithelial cells are well documented in literature [reviewed in: 10]. Here, we extended our previous question, namely asking whether Taar1-mediated signalling affects cathepsin activities such as seen in a knock-out mouse model [8], by deciphering whether Taar1 function at the apical plasma membrane of thyrocytes is directly linked to cysteine cathepsin activities. Therefore, we designed an *in vitro* study using FRT cells featuring one Taar1-positive primary cilium per cell [1,11,12]. Localization of Taar1 and the principal formation of primary cilia were studied by immunofluorescence, also including cells depleted of cholesterol-rich domains because those are thought to constitute cilia [13]. To enable determination of the precise sub-cellular localization, high-resolution confocal laser scanning microscopy (LSM) and z-stacking were applied. Furthermore, cathepsin activities were assessed and inhibited by activity based probes (ABP) designed by us and protease inhibitors for broad-spectrum and specific inhibition [14–17]. The results revealed that cathepsin B and L activity is required for maintenance of a fully differentiated state of thyrocytes featuring Taar1-bearing primary cilia.

2. Materials and methods

2.1. Cell culture

Rat thyrocytes, namely the FRT and FRTL-5 cell lines [11,12], were grown at 37 °C with 5% CO₂ in a moisturized atmosphere. FRT and FRTL-5 cells were cultured in Coons F-12 medium (Sigma-Aldrich Chemie GmbH, Steinheim, Germany), which contained 2.68 mg/mL sodium bicarbonate and 5% fetal bovine serum (FBS) (Sigma-Aldrich Chemie GmbH, Taufkirchen, Germany, #F7524). This medium was supplemented with a hormone mixture, consisting of 2 µg/mL insulin (Sigma-Aldrich Chemie GmbH, #I6634), 20 ng/mL Gly-His-Lys complex (Sigma-Aldrich Chemie GmbH, #G7387), 3.62 ng/mL hydrocortisone (Sigma-Aldrich Chemie GmbH, #H0135), 5 µg/mL transferrin (Invitrogen, Darmstadt, Germany, #11107–018) and 10 ng/mL somatostatin (Sigma-Aldrich Chemie GmbH, #S1763). FRTL-5 cell culture media were additionally supplemented with 1 mU/mL TSH (Sigma-Aldrich, #T-8931).

2.2. RT-PCR

An RNeasy Mini Extraction Kit (Qiagen, Hilden, Germany, #74106) was used for total RNA extraction from FRT and FRTL-5 cells, which was used as a template for cDNA synthesis. Each reaction was allowed to proceed for 60 min at 37 °C and contained 10 µg of total RNA, 0.5 mM dNTPs, 1 µM of rat Taar1 anti-sense primer (instead of Oligo dT) and 4 U of reverse transcriptase. The PCR reactions on synthesized cDNA were performed at an annealing temperature of 60 °C, using the following primers at 0.5 µM, each, for rat Taar1: Taar1 sense 5'-GTGAGAACAGTTGAGCA-3 and 5'-

CGCAGGCAGAAGACCTGATT-3' anti-sense [18], respectively, 0.2 mM dNTPs, 0.9 mM MgCl₂, and 2 U Taq DNA polymerase (all from MBI Fermentas, St. Leon-Rot, Germany). RT-PCR products were separated through 1.5% agarose gel electrophoresis and visualized by incubation with 0.3% ethidium bromide. A FastRuler™ Low Range DNA Ladder (Thermo Fisher, Bonn, Germany, #SM1103) was used as a size marker.

2.3. Protease activity and protein biosynthesis inhibition experiments

Cathepsins B and L, as well as all cysteine peptidase activities, were inhibited in confluent cell cultures of FRT and FRTL-5 cells by incubation with 10 µM CA-074 (Calbiochem, Darmstadt, Germany, #205530), 10 µM cathepsin L Inhibitor III (Calbiochem, #219427), or 10 µM E64 (Enzo Life Sciences, Lörrach, Germany, #BML-PI 107–0001), respectively, for 8 h, under otherwise standard cell culture conditions. As a vehicle control, DMSO (0.1% final concentration) was used. In additional experiments, protein *de novo* biosynthesis was blocked by co-treatment with 1 µg/mL cycloheximide (Sigma-Aldrich Chemie, #C7698) and protease inhibitors for 8 h. Efficiency of protein *de novo* biosynthesis was monitored by determination of the protein amounts of procathepsin L.

2.4. Labelling of lysosomes with LysoTracker red DND-99

In analogy to previous experiments with FRT cells [1], confluent grown FRTL-5 cells were washed with PBS for 2 min at 37 °C and incubated with 1 µM LysoTracker Red DND-99 (Molecular Probes, Leiden, Netherlands, #L-7528) in serum-free culture medium for 45 min at 37 °C. Afterwards, cells were washed twice with complete culture medium for 3 min each at 37 °C, followed by a chase period of 30 min in complete cell culture medium at 37 °C. Cells were then washed with culture medium twice for 3 min each, before they were fixed with 4% paraformaldehyde in 200 mM HEPES, at pH 7.4, for 20 min at room temperature and stained as described below.

2.5. Activity-based probes

Protease inhibitor-treated FRT and FRTL-5 cells were washed with PBS for 2 min at 37 °C, followed by incubation in serum-free medium containing 10 µM of a pan-specific ABP for cysteine peptidases, namely DCG-04 Red [14], or a cathepsin B-selective ABP, namely NS-173 [15], for 30 min at 37 °C. Afterwards, cells were washed with complete culture medium twice for 3 min each at 37 °C, followed by a chase period of 30 min in complete cell culture medium at 37 °C. Cells were then washed with culture medium twice for 3 min each, and fixed with 4% paraformaldehyde in 200 mM HEPES, at pH 7.4, for 20 min at room temperature. Nuclear DNA was counter-stained with 5 µM Draq5™ (Biostatus Limited, Shepshed, Leicestershire, UK) for 15 min at room temperature. Before mounting, cells were washed three times for 5 min each with calcium- and magnesium-free PBS (CMF-PBS) and rinsed in de-ionized water. The cells were then mounted with an embedding medium consisting of 33% glycerol and 14% Mowiol (Hoechst AG, Frankfurt, Germany) in 200 mM Tris-HCl at pH 8.5.

2.6. Cholesterol depletion by β -cyclodextrin treatment

The stability of primary cilia of FRT cells was challenged by incubation of confluent grown cultures with the cholesterol-depleting agent β -cyclodextrin (Sigma-Aldrich Chemie GmbH, #C4767). Confluent FRT cell cultures were washed with PBS at

37 °C, and incubated for 8 h with 10 mM of β -cyclodextrin in serum-free medium, under otherwise standard cell culture conditions.

2.7. Indirect immunofluorescence and cell surface staining

Protease inhibitor-, cycloheximide-, LysoTracker Red DND-99-, ABP-, and/or β -cyclodextrin-treated cells were fixed with 4% paraformaldehyde in 200 mM HEPES, at pH 7.4, for 20 min at room temperature. Next, cells were washed three times for 5 min with CMF-PBS, composed of 0.15 M NaCl, 2.7 mM KCl, 1.5 mM NaH_2PO_4 , and 8.1 mM Na_2HPO_4 , at pH 7.4, followed by blocking with 3% bovine serum albumin (BSA; Carl Roth GmbH, Karlsruhe, Germany) in CMF-PBS for 1 h at 37 °C. Primary antibodies used in this study, namely goat anti-mouse cathepsin B (Neuromics, Hiddenhausen, Germany, #GT15047, 1:100), goat anti-mouse cathepsin L (Neuromics, #GT15049, 1:100), rabbit anti-mouse Taar1 (Antibodies Online, Aachen, Germany, #ABIN 351020, 1:50), mouse anti-rat acetylated α tubulin (Sigma-Aldrich Chemie GmbH, #T7451, 1:50), polyclonal mouse anti-human Lamp2 (DSHB, #H4B4, 1:50), and polyclonal mouse anti-human Golgin97 (Molecular Probes, #A-21270, 1:50) were diluted in 0.1% BSA in CMF-PBS. Primary antibody incubation was performed for 16 h at 4 °C. Afterwards, cells were washed 6 times for 5 min with 0.1% BSA in CMF-PBS, followed by incubation with Alexa 488- or Alexa 546-conjugated secondary antibodies (Molecular Probes, Karlsruhe, Germany, #A21085, #A11070, #A11018, 1:200) for 1 h at 37 °C, in the presence of 5 μM Draq5TM (Biostatus Limited) to counter-stain nuclear DNA. Specificity of secondary antibodies was confirmed by omitting primary antibodies. Specificity of the rabbit anti-mouse Taar1 antibodies was verified previously using Taar1-deficient thyroid tissue [1].

In some experiments, glycosylated plasma membrane constituents were stained with 10 $\mu\text{g}/\text{mL}$ of the biotinylated lectin Concanavalin A obtained from *C. ensiformis* (ConA; Sigma-Aldrich Chemie GmbH, #C2272) for 30 min at 4 °C, followed by incubation with Alexa Fluor[®] 546-conjugated streptavidin (Molecular Probes, Karlsruhe, Germany, #S-11225) as the secondary ConA detection label. Before mounting, cells were washed three times for 5 min each with CMF-PBS and rinsed in de-ionized water. The cells were then mounted with an embedding medium consisting of 33% glycerol and 14% Mowiol (Hoechst AG, Frankfurt, Germany) in 200 mM Tris-HCl at pH 8.5.

2.8. Image acquisition

Immunolabeled, ConA-stained, and ABP-probed cells were visualized with a confocal laser scanning microscope equipped with Argon and Helium–Neon lasers (LSM 510 Meta; Carl Zeiss Jena GmbH, Jena, Germany). Images were obtained at a pinhole setting of one Airy unit and at a resolution of 1024×1024 pixels. Micrographs were analyzed with the LSM 510 software, release 3.2 (Carl Zeiss Jena GmbH). In some experiments, immunolabeled cells were imaged using a conventional fluorescence microscope (Carl Zeiss Jena GmbH).

2.9. Image analysis and quantification of different Taar1 localization patterns

CellProfiler 2.1.1 (version 2.1.1.; available from the Broad Institute at www.cellprofiler.org [19]) was used to determine the ratio of FRT cells displaying localization of Taar1 at primary cilia, or in compartments of the secretory pathway, to all cells. In addition, the fluorescence intensity of DCG-04 Red-positive signals, normalized to the number of cells, in protease inhibitor-treated FRT cells, was also quantified by using CellProfiler-based pipelines. The diameters

of Taar1- or cathepsin L- and acetylated α tubulin-positive primary cilia, respectively, were determined morphometrically using the LSM 510 software.

2.10. TCA protein precipitation from conditioned media

Conditioned media of post-confluent cultures of FRT cells were collected after 24 h from 10-cm dishes. Conditioned media were centrifuged at 200 g for 10 min at 4 °C in order to remove dead cells and cell debris. The cleared conditioned media were then incubated with ice-cold trichloroacetic acid (TCA, 10% final concentration) for 60 min at 4 °C, followed by centrifugation at 13,000 g for 10 min at 4 °C. The supernatants were discarded, and pellets were dried in an Eppendorf[®] centrifugal vacuum concentrator (Sigma-Aldrich Chemie GmbH, #Z368172) for 15 min. The pellets were resuspended in SDS-PAGE sample buffer (10 mM Tris-HCl, pH 7.6, 0.5% SDS, 25 mM DTT, 10% glycerol and 25 $\mu\text{g}/\text{mL}$ bromophenol blue). The pH was adjusted by adding 1 μL of 1.5 M Tris-HCl, pH 8.8, dropwise, until the color of the solution turned from yellow to blue, before filling up with sample buffer completely. Samples were adjusted to equal protein concentrations of the corresponding cell lysates (see below), respectively, before the TCA-precipitated proteins were separated on SDS-PAGE-gels.

2.11. Protein lysate preparation

All steps were performed on ice and centrifugations at 4 °C. The FRT cells treated with protease inhibitors were washed three times for 1 min, each, with ice cold PBS before detachment with a cell scraper and collection by centrifugation at 200g for 5 min. For determination of the amounts of cellular versus secreted cathepsins, the same procedure was performed with cells after collection of the 24 h-conditioned media (see above). Afterwards, cells were resuspended in lysis buffer (20 mM Na_2HPO_4 , 50 mM NaCl, 0.5% Triton X-100, pH 7.4), and incubated for 30 min at 4 °C on an end-over-end rotor. The supernatants were cleared through centrifugation for 10 min at 13,000 g and 4 °C, and stored at -20 °C. Protein sample concentrations were determined by the Neuhoff assay [20].

2.12. Cathepsin B and L activity assays

Cathepsin B and L activity assays were performed as describe before [9,21,22]. Protein samples prepared from protease inhibitor-treated FRT cells were assayed by monitoring cleavage of 10 μM cathepsin B-specific substrate N-benzoyloxycarbonyl-arginine-arginine-7-amido-4-methylcoumarin hydrochloride Z-Arg-Arg-AMC^{*}HCl (Bachem, Bubendorf, Switzerland, #I-1135) or 10 μM cathepsin L-specific substrate N-benzoyloxycarbonyl-phenylalanyl-arginine-7-amido-4-methylcoumarin Z-Phe-Arg-AMC (Bachem, Bubendorf, Switzerland, #I-1160) at pH 6.0, and for 60 min at 40 °C. In addition, 10 μM of CA-074 (Calbiochem, #205530) was added to the samples incubated with Z-Phe-Arg-AMC, to prevent the substrate's proteolysis by cathepsin B. Samples incubated with Z-Phe-Arg-AMC with addition of 10 μM CA-074 and 10 μM cathepsin L Inhibitor III were used for adjustment of background readings in cathepsin L activity assays. In parallel, in negative controls prepared for each sample, 10 μM E64 was added at the start of the reaction time. Substrate cleavage was stopped by the addition of 2 M TrisHCl (pH 9.0). The amounts of released AMC were quantified by measuring the fluorescence with a Tecan GENios Reader (Tecan Deutschland GmbH) using an excitation wavelength of 360 nm and emission reading at 465 nm.

2.13. SDS-PAGE, immunoblotting, and quantification of the proportions of cell-associated and secreted cathepsins

Proteins were separated through SDS-PAGE on 12.5% polyacrylamide gels along with a PageRuler Prestained Protein ladder (Thermo Scientific, #26616) and transferred onto nitrocellulose membranes by semi-dry blotting. Unspecific binding sites were blocked with 5% milk powder in PBS, supplemented with 0.3% Tween (PBS-T) for 16 h at 4 °C. Afterwards, membranes were incubated for 2 h at room temperature with specific antibodies, namely goat anti-mouse cathepsin B (Neuromics, #GT15047, 1:1000), goat anti-mouse cathepsin L (Neuromics, #GT15049, 1:1000), and rabbit anti-human β tubulin antibodies (Abcam, #ab6046, 1:1000), diluted in PBS-T. Incubation with horseradish peroxidase-conjugated secondary antibodies (Southern Biotech, Birmingham, USA, #6160-05, #4050-05, 1:5000) was performed for 1 h at room temperature, followed by incubation with the horseradish peroxidase substrate (Pierce, Rockford, USA), and visualization through enhanced chemiluminescence onto XPosure films (Thermo Scientific).

For quantification of the proportions of secreted and cell-associated cathepsins, chemiluminescence signals were detected using the Li-Cor system (LI-COR Biosciences, Lincoln, Nebraska, USA) to avoid over-exposure. Signal intensities were then quantified from individual bands upon background subtraction using the software Image Studio Lite, version 5.2. Approx. 1.5% and 5.5% of all available protein per dish were separated by SDS-PAGE for determinations of cell-associated and secreted proteins, respectively. Therefore, dilution factor correction was used to calculate the final balances of the proportions of total protein for each, procathepsins, single and heavy chains of the two-chain forms. For documentation purposes, the immunoblots were additionally visualized onto XPosure films as explained above.

2.14. Statistical analysis

Data analysis was performed by the use of GraphPad Prism 5.01 software (GraphPad, San Diego, California, USA). The same software was used for determination of levels of significance by one-way ANOVA, followed by Tukey *post hoc* test.

3. Results

Previously, sub-cellular localization of Taar1, as well as extra-cellular cathepsin L, was found to be confined to the primary cilia of well-polarized FRT cells [1] and primary thyrocytes [9], respectively. Moreover, Taar1 deficiency in mice resulted in decreased cysteine cathepsin activities [8]. Hence, potential interaction of sub-cellular localization of Taar1 with proteolytic activity of cysteine cathepsins in rat thyroid epithelial cells was analyzed in this study. As cellular models, the structurally differentiated FRT cells, which lack thyroid stimulating hormone (TSH) receptors, and the functionally differentiated, TSH receptor-bearing FRTL-5 cells were used.

3.1. Taar1 is expressed in thyroid epithelial cell lines

Total RNA was isolated from FRT and FRTL-5 cells and used as a template for cDNA synthesis, followed by PCR amplification with Taar1-specific primers. The expected products with sizes of 296 bps were detected in agarose gels, confirming Taar1 expression in the cell lines investigated herein (Fig. 1, A-B, lanes 3–5). As Taar1 is encoded by an intron-less gene, contamination of RNA samples with genomic DNA might cause false-positive results [23]. In order to exclude contamination of samples with genomic DNA, control

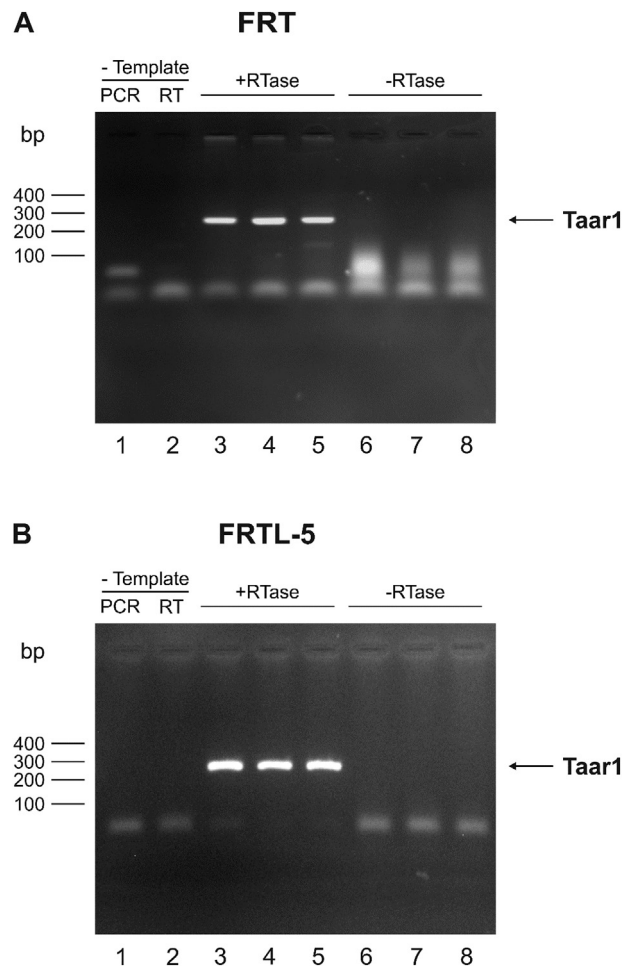


Fig. 1. Taar1 expression in FRT and FRTL-5

Taar1 was amplified from cDNA templates of FRT and FRTL-5 cells (A-B, lanes 3–5). Control experiments were conducted in which reverse transcriptase (lanes 6–8) or template (lanes 1 and 2) was omitted. Note that bands with expected sizes of 296 bps were observed in samples containing template and reverse transcriptase (A-B, lanes 3–5).

experiments were conducted, in which reverse transcriptase was excluded (Fig. 1, A-B, lanes 6–8). No bands were observed in the control experiments, indicating purity of RNA samples and cDNA preparations yielding Taar1-specific amplicons.

3.2. Taar1 and cathepsin L are co-localized at the primary cilium of FRT cells

While Taar1 is following the secretory pathway to reach primary cilia of thyrocytes [1], cathepsins are recruited out of endo-lysosomes for retrograde trafficking and subsequent secretion and re-association with the plasma membrane [24,25]. Hence, here we aimed to test for possible co-localization of Taar1 with cathepsins B or L at the cilia of FRT cells. Double labelling of well-polarized FRT cells with rabbit anti-mouse Taar1 and goat anti-mouse cathepsin B or L antibodies, respectively, revealed co-localization of Taar1 with cathepsin L (Fig. 2, B, arrows, yellow signals), but to a much lesser extent with cathepsin B (Fig. 2, A, arrows, green signals) at the primary cilia. It is of interest to note that Taar1 was not co-localized with any of the two proteases in intra-cellular compartments, i.e. endo-lysosomes (Fig. 2, A' and B', arrowheads).

Cilia of FRT cells were also analyzed morphometrically, revealing

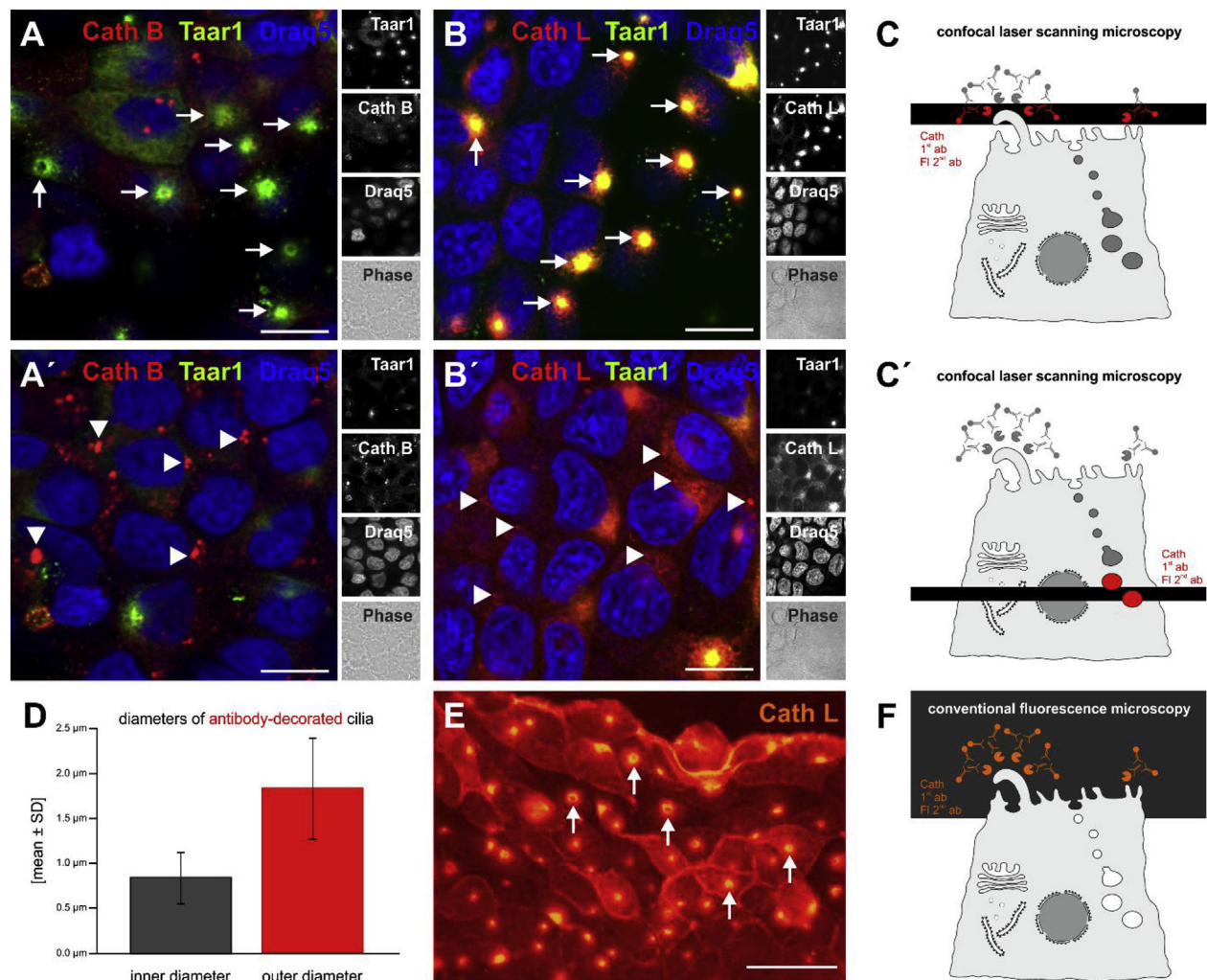


Fig. 2. Co-staining of Taar1 and cathepsin B or L in FRT cells

Confocal laser scanning (A-B') and conventional micrographs (E) of FRT cells immunolabelled with rabbit anti-mouse Taar1 antibodies (A-B', green signals), and with goat anti-mouse cathepsin B (A and A', red signals), or goat anti-mouse cathepsin L (B, B', and E, red signals), respectively. Single confocal sections were taken at the top (A and B) and median poles (A' and B') of FRT cells, respectively, schematic drawings of FRT cells (C and C') indicate where optical sections were positioned. Single channels, overlays of different channels, and corresponding phase contrast micrographs are depicted as indicated. Morphometry was performed to determine the inner and outer diameters of antibody-decorated cilia (D). The extended depth of focus in conventional microscopy (E) allows visualization of cilia and microvilli-associated cathepsin L at the apical surface of FRT cells as sketched in F. Arrows in A-B' and E denote cilia, while arrowheads point to endo-lysosomes. Nuclei were counter-stained with Draq5™ (A-B', blue signals). Scale bars represent 10 μm in A-B' and 50 μm in E.

an inner diameter of the Taar1-positive structures of $0.80 \pm 0.29 \mu\text{m}$ (Fig. 2, D). The outer diameter of anti-Taar1-decorated cilia was much larger because an indirect immunostaining protocol was used, which resulted in signal enhancement and enlargement of the fluorescent structures to $1.86 \pm 0.57 \mu\text{m}$ (Fig. 2, D and C).

Conventional fluorescence microscopy allows for imaging with a focal depth larger than in confocal sections (Fig. 2, F cf. C). Thus, cell surface-associated structures of immunostained FRT cells were analyzed comprehensively by conventional fluorescence microscopy, demonstrating one cathepsin L-decorated cilium present in most if not all FRT cells (Fig. 2, E, arrows) in addition to staining of numerous microvilli-like surface extensions.

The results indicated that cathepsin L, in particular, was secreted in high enough amounts to re-associate with primary cilia at the apical plasma membrane of FRT cells to become detectable by immunolabeling. In order to gain further information on the molecular forms of secreted cathepsins, proteins were TCA-precipitated from conditioned media of confluent FRT cultures and immunoblotted using cathepsin-specific antibodies. The

respective cell lysates were analyzed in parallel with the proteins in conditioned media, and on the same blots, in order to determine the percentages of total protein per dish for each distinct cell-associated or secreted cathepsin form.

Cathepsins are synthesized as proforms at the rough endoplasmic reticulum (rER), followed by trafficking to the Golgi apparatus with further destination to late endosomes, where the propeptide is cleaved to give rise to the mature forms of cathepsins. Hence, when goat anti-mouse cathepsin B antibodies were used, bands representing the heavy chain of two chain and the single chain form of cathepsin B, respectively, were detectable in the cell lysates (Fig. 3, A, lanes 1–3). The TCA precipitates of two of the three corresponding conditioned media contained bands representing procathepsin B (Fig. 3, A, lanes 5 and 6), while mature cathepsin B was only detectable in over-exposed blots (not shown). All forms of cathepsin L, namely the pro-, single chain, and two chain forms were detectable in the cell lysates (Fig. 3, B, lanes 1–3) with the mature forms being most prominent as expected. In contrast, only small amounts of heavy chain but high amounts of

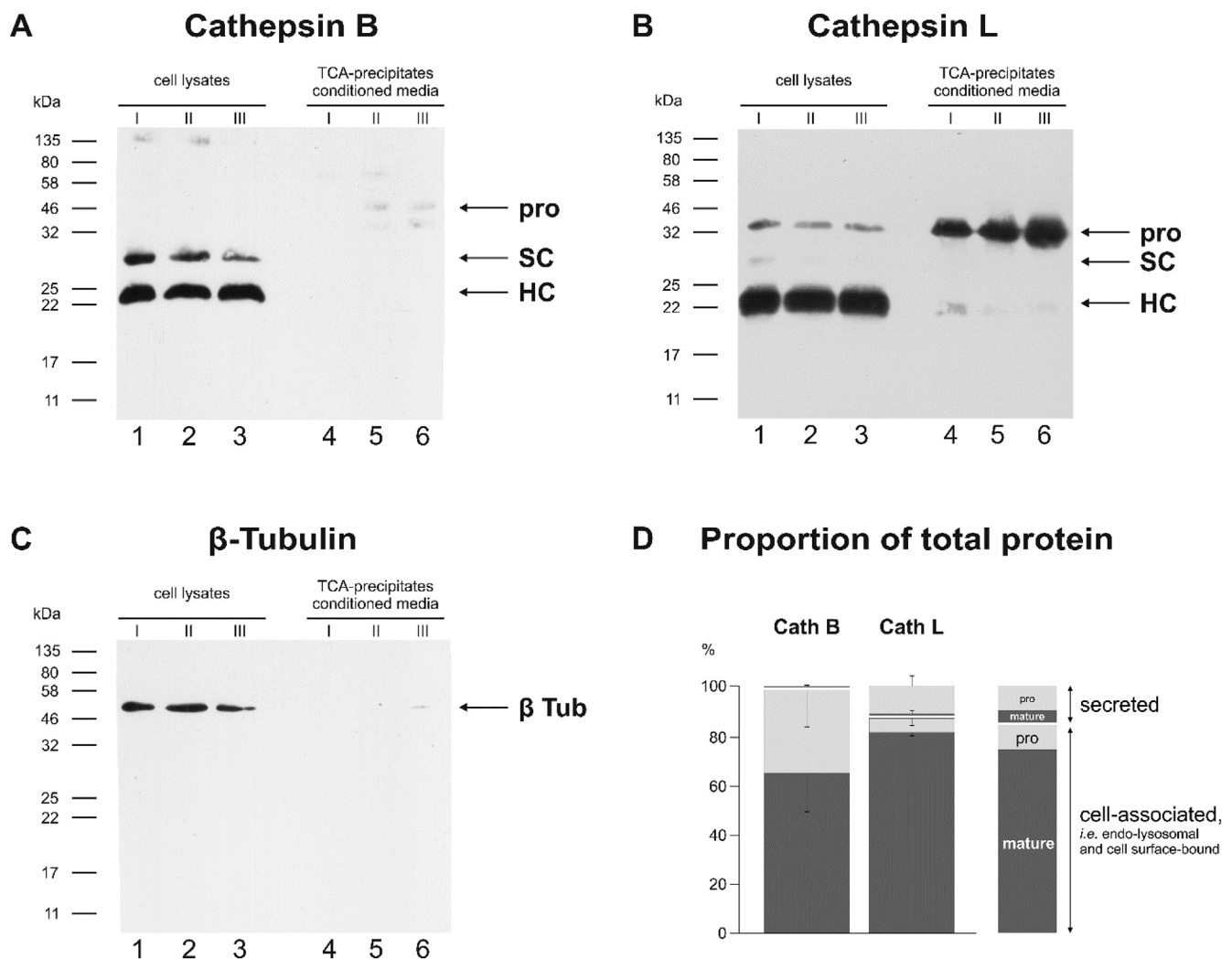


Fig. 3. Cathepsin B and L secretion from FRT cells

Proteins precipitated with TCA from the 24 h conditioned media collected from the apical pole of confluent FRT cell cultures and corresponding cell lysates I–III, respectively, were immunoblotted with anti-cathepsin B or L antibodies (A and B), and upon stripping, the identical membranes were reacted with rabbit anti-human β -tubulin antibodies (C). The amounts of secreted and cell-associated cathepsin forms, namely, the proform (pro), single chain (SC) and the heavy chain of two chain cathepsins (HC) were quantified by densitometry and are given as means plus and minus standard deviations calculated from the corresponding percentages of total protein (D), respectively. Molecular mass markers are indicated in the left margins of A–C.

procathepsin L were found to be secreted from FRT cells cultured in tight monolayers (Fig. 3, B, lanes 4–6). The membranes were stripped off antibodies, and then incubated with rabbit anti-human β -tubulin antibodies in order to exclude the possibility of contamination of media precipitates with cell residues. Bands at approx. 55 kDa were detected in the cell lysates (Fig. 3, C, lanes 1–3), while a very faint band corresponding to β -tubulin was observed in only one of three conditioned media precipitates (Fig. 3, C, lanes 4–6), confirming that the proteins precipitated from the conditioned media of FRT cells represented secreted proteins.

The relative proportions of secreted and cell-associated pro- and mature cathepsins B and L were determined upon densitometry of the respective bands, indicating that less than 1% of cathepsin B but approx. 12% of cathepsin L were present in the conditioned media of FRT cells (Fig. 3, D). This data supports the notion of cathepsin L secretion rates exceeding those of cathepsin B in confluent FRT cell cultures. It should be noted, however, that cilia- or microvilli-associated cathepsins are determined with the cell-associated fractions. Thus, it is difficult to conclude on the amounts of cathepsins that, upon secretion, are re-associated with cilia at the FRT

cell surface, where they eventually act as proteolytically active enzymes despite the low amounts detectable by biochemical means [9].

3.3. Inhibition of cathepsin B and L activities in monolayer cultures of FRT cells

Proteolytically active cysteine cathepsins were visualized upon incubation with the activity based probe (ABP) DCG-04 Red, a pan-specific ABP for cysteine peptidases [14]. Control FRT cell cultures revealed numerous puncta over cellular profiles, resembling endo-lysosomes, while occasionally also dots in ring-like assemblies were discernible, i.e. reminiscent of cilia appearances (Fig. 4, A, arrows). The proteolytic activities of cathepsins were inhibited in FRT cells via treatment with the cathepsin B inhibitor CA-074, the cathepsin L inhibitor III, and with the broad spectrum cysteine peptidase inhibitor E64. Specificity of these inhibitors was shown by us [26,27] and others before. The fluorescence intensity of DCG-04 Red per cell was found to be decreased in samples that were pre-treated with cathepsin inhibitors (Fig. 4, B–D, cf. A, and F),

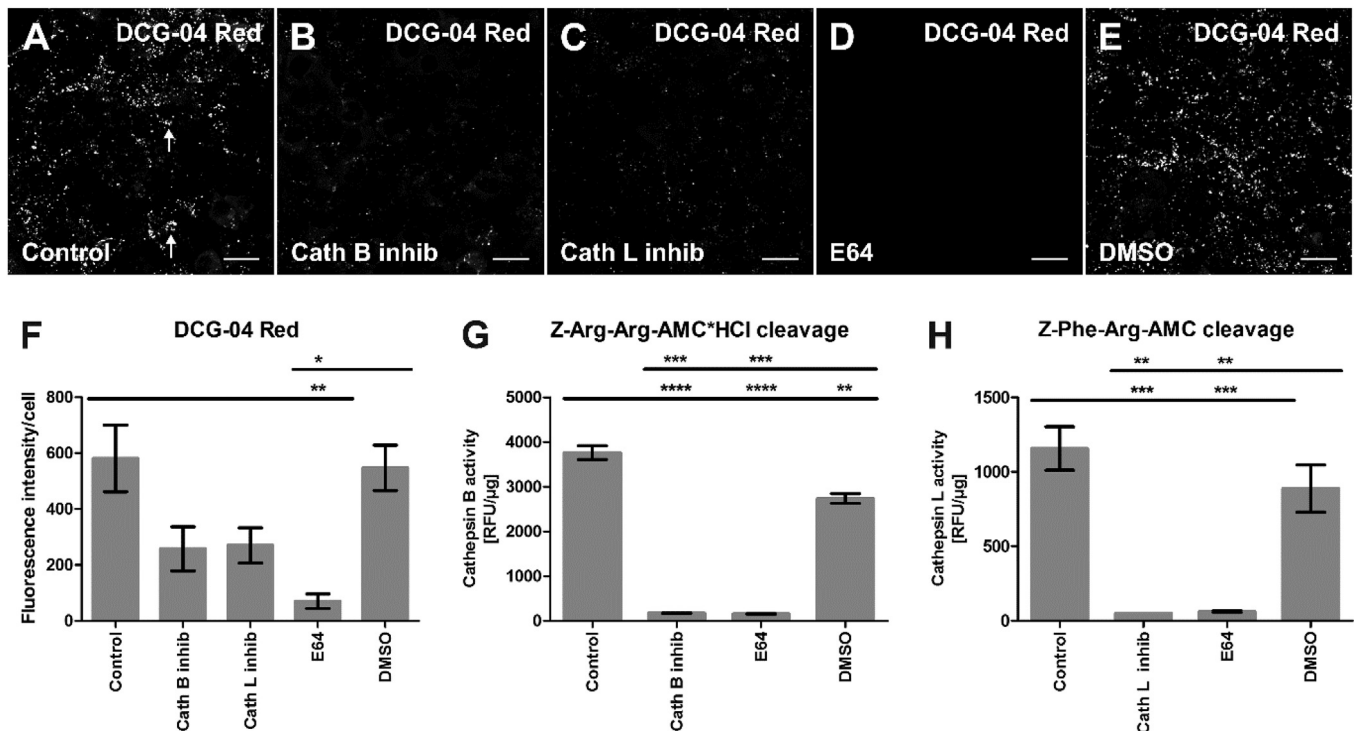


Fig. 4. Inhibition of proteolytic activity of cysteine peptidases in FRT cells

FRT cells treated with cathepsin B or L inhibitors, E64, and controls (as indicated) were incubated with 10 μ M DCG-04 Red (A–E). Single confocal sections were taken at the median poles of FRT cells and the fluorescence intensity of DCG-04 Red was measured by densitometry (F). Cathepsin activities were determined as relative fluorescence units (RFU) per protein by cleavage of Z-Arg-Arg-AMC*HCl and Z-Phe-Arg-AMC as cathepsin B- and L-selective substrates (G and H), respectively, confirming that cathepsin inhibitions were specific and complete.

Scale bars in A–E represents 10 μ m; arrows in A points to cilia-like appearances of ABP-visualized cathepsin activities in control cells. Data are depicted as means \pm standard deviations, * P < 0.05, ** P < 0.01, *** P < 0.001, **** P < 0.0001. Number of cells probed with DCG-04: Control n = 775, Cath B inhib n = 616, Cath L inhib n = 553, E64 n = 510, DMSO n = 683.

suggesting that inhibitor treatment indeed resulted in inhibition of the proteolytic activities of cathepsins. DMSO treatment served as solvent control and was comparable to non-inhibited controls (Fig. 4, E cf. A, F).

Next, we verified accuracy of cathepsin B and L inhibition through activity assays performed with cell lysates, prepared from inhibitor-treated FRT cell cultures, and non- or DMSO-treated controls. The activity of cathepsins B and L was indeed inhibited in inhibitor-treated samples, as is shown by the lack of cleavage of their specific substrates, respectively (Fig. 4G and H). Cathepsin B and L activities were also inhibited in E64 treated samples (Fig. 4G and H) as expected. DMSO treatment caused a significant decrease in cathepsin B activity in comparison to non-treated cells. However, the proteolytic activity of cathepsin B of the vehicle control was still significantly higher than that of cathepsin B inhibitor-treated cells (Fig. 4, G). Lastly, there was no significant difference in proteolytic activity of cathepsin L between non-treated and DMSO vehicle controls (Fig. 4, H).

3.4. Taar1 localization is confined to compartments of the secretory pathway upon inhibition of cathepsin B or L activity in FRT cells

In order to study the possible importance of cysteine cathepsin activity for the sub-cellular localization of Taar1 and its presence at primary cilia, the proteolytic activity of cathepsins was first inhibited, and the sub-cellular localization of Taar1 was then determined in FRT cells upon fixation and immunolabeling. Cathepsin B inhibitor-treated cells were thought to serve as controls as cathepsin B was not strongly co-localized with Taar1 at the primary cilia of FRT cells. It is important to note that Taar1

localization in FRT cells is heterogeneous as observed before [1], and accordingly, Taar1 was observed at the primary cilium of some and in compartments of the secretory pathway of other FRT cells in any given monolayer (Fig. 5, A and A', respectively). Localization of Taar1 at primary cilia was judged from their identification as acetylated α -tubulin-positive structures (Fig. 5, green and red signals, respectively, yielding yellow signals when co-localized, arrows), while Taar1-positive secretory pathway compartments appeared reticular as previously described [1].

In non-treated samples and vehicle controls, Taar1 was localized at the primary cilium in over 85% of the cells analyzed (Fig. 5, A and E, arrows, G), while only 15% of the FRT cells were characterized by Taar1 localization in compartments of the secretory pathway (Fig. 5, A' and E', G). Upon inhibition of cathepsin L activity and E64 treatment, this ratio was inverted such that 85% of the cells were found to contain Taar1-positive signals in the compartments of the secretory pathway (Fig. 5, C' and D', arrowheads and insets, G), while Taar1 remained at cilia in only 15% of inhibitor-treated cells. Cathepsin B activity inhibition resulted in an even more pronounced effect, such that almost 95% of the cells were characterized by localization of Taar1 in compartments of the secretory pathway (Fig. 5, B', arrowheads and inset, G). However, there were no significant differences between the various inhibitor treatments, which all resulted in Taar1 redistribution to the rER, which was in particular obvious from nuclear envelope labelling in inhibitor-treated cells at the respective focal plane (Fig. 5, B'–D', insets). In addition, co-localization of Taar1 staining with that of the cilium marker mouse anti-rat acetylated α -tubulin was no longer revealed in most of the inhibitor-treated cells as judged from the infrequency of yellow signals at either focal plane, namely at the cells'

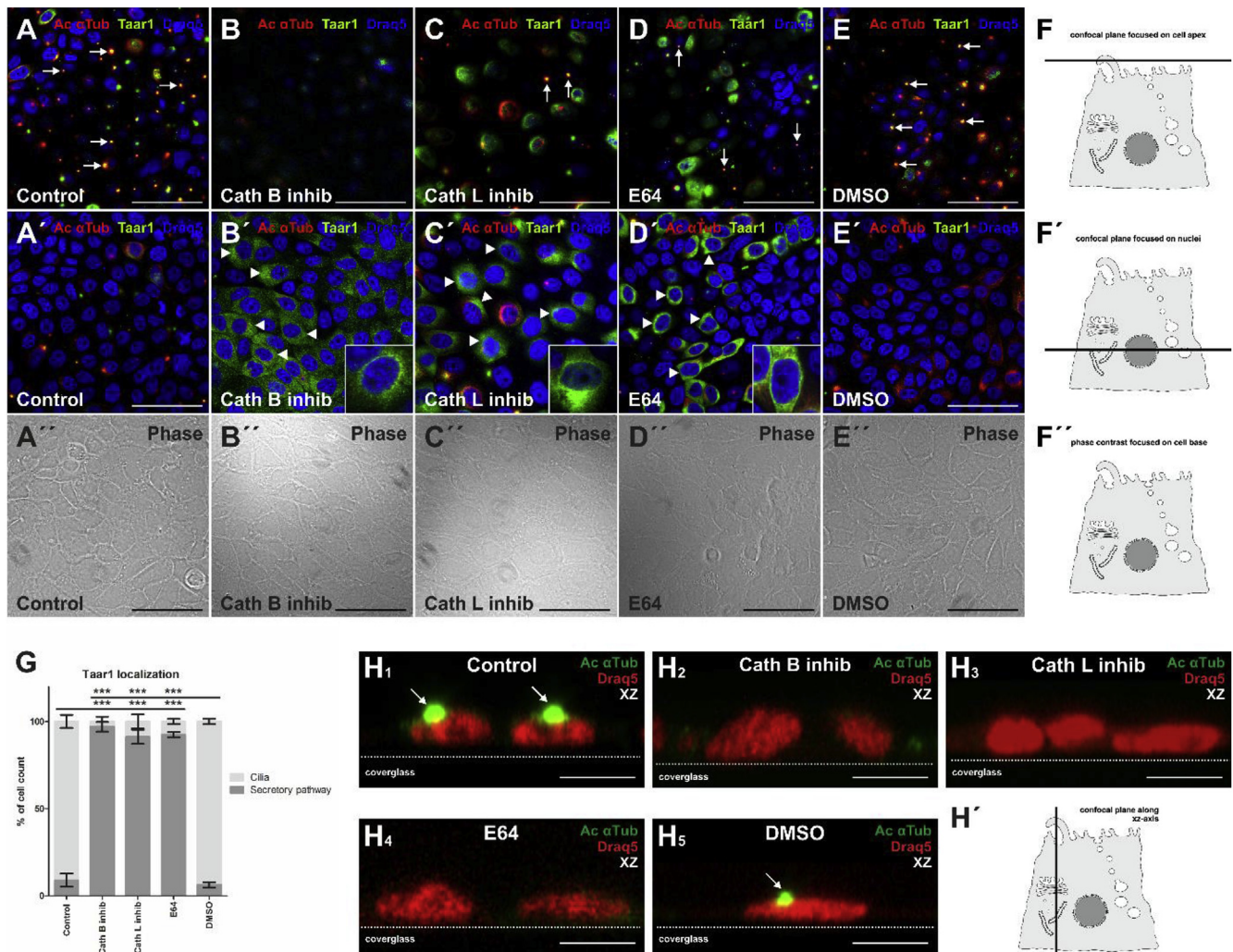


Fig. 5. Sub-cellular localization of Taar1 in FRT cells treated with cathepsin inhibitors

FRT cells treated with cathepsin inhibitors (as indicated) and controls were stained with anti-Taar1 (green signals) and anti-acetylated α -tubulin antibodies (red signals). Corresponding phase contrast images are shown in A''-E'', respectively. Sketches in F and F' denote where optical sections were positioned. The graph (G) represents the proportion of FRT cells characterized by sub-cellular localization of Taar1 confined to the compartments of the secretory pathway (dark grey), or at primary cilia (light grey). Representative scans along xz as indicated in H' are shown in H1-H5, in which cells were stained with anti-acetylated α -tubulin antibodies (green signals) and Draq5TM visualizing nuclear DNA (red signals).

Taar1 was localized mostly in the primary cilium of non- and DMSO-treated FRT cells (A and E, H1 and H5, arrows), and in compartments of the secretory pathway in cathepsin B and L inhibitor- and E64-treated cells (B', C', and D', arrowheads). Localization in the rER is inferred from anti-Taar1-positive stainings of the nuclear envelope (B'-D', insets). Scale bars represent 50 μ m. Data are depicted as means \pm standard deviations, ***P < 0.001. Numbers of cells analyzed via immunofluorescence: Control n = 2193, Cath B inhib n = 1733, Cath L inhib n = 2053, E64 n = 535, DMSO n = 1751.

apex and across the nuclei (Fig. 5, B-D and B'-D', respectively). Presence or absence of cilia can also be appreciated from the respective xz-scans (Fig. 5, H1-H5 and H').

The results indicated that cysteine peptidase activity is important to maintain localization of Taar1 at primary cilia of FRT cells. In addition, the absence of acetylated α -tubulin-positive cilia from the apices of the majority of inhibitor-treated cells and appearance of acetylated α -tubulin-positive tubular networks around the nuclei indicated that cysteine peptidase activity is important to maintain cilia of FRT cells intact altogether.

3.5. Localization of Taar1 in the secretory pathway upon cathepsin activity inhibition is not affected by inhibition of *de novo* protein biosynthesis

Testing whether Taar1 is present predominantly in the rER and other compartments of the secretory pathway upon cathepsin B or

L inhibition due to increased *de novo* biosynthesis, we blocked protein biosynthesis by cycloheximide co-treatment with cathepsin inhibitors. Thus, FRT cells were incubated with cathepsin inhibitors for 8 h in the presence of 1 μ g/mL cycloheximide. Cathepsin inhibitor-treated FRT cells without addition of cycloheximide were used as controls for this experiment (not shown).

We assumed that co-treatment of FRT cells with cathepsin inhibitors and cycloheximide could result in alterations of Taar1 localization. However, we did not observe any differences in the effect of protease-inhibitor treatment on the re-location of Taar1 from cilia to compartments of the secretory pathway between cycloheximide and inhibitor co-treated samples (Fig. 6, A-E', green signals, and G) and cultures in which no cycloheximide was used (see Fig. 5, A-E', green signals, and G). Additionally, the previously observed disappearance of primary cilia upon inhibitor treatment was also observed in cultures that were pre-treated with cycloheximide, while the controls maintained cilia (Fig. 6, A-E', red

signals).

In order to confirm inhibition of *de novo* protein biosynthesis in the experimental setting, proteins were isolated from FRT cells following the protease inhibitor and cycloheximide co-treatment, and immunoblotted with goat anti-mouse cathepsin L antibodies (Fig. 6, H). The band representing the proform of cathepsin L was absent in lysates obtained from cycloheximide-treated cells, thereby confirming that *de novo* synthesis of proteins was blocked by incubation with 1 µg/mL of cycloheximide (Fig. 6, H) in controls, vehicle-treated cells and in the presence of protease inhibitors alike. Thus, the results indicated that it was pre-existing Taar1, which was re-located from a primary cilia-based to a predominant localization in secretory compartments of FRT cells upon treatment with cathepsin B and L inhibitors or E64.

3.6. Taar1 is retained in the compartments of the secretory pathway upon β-cyclodextrin treatment

The data above showed that Taar1 localization was dependent

on cysteine cathepsin activities. In addition, in cathepsin inhibitor-treated cells, primary cilia were not formed properly, or were not maintained. Thus, cathepsin inhibitor treatment caused a relocation to and retention of Taar1 in compartments of the secretory pathway, accompanied by the disappearance of primary cilia. Therefore, next we aimed to further confirm that Taar1 was retained in compartments of the secretory pathway of FRT cells due to a lack of primary cilia. In order to disrupt primary cilia, FRT cells were treated with β-cyclodextrin, which is a small amphipathic, cyclic oligosaccharide, composed of seven glucose monomers with cholesterol-chelating abilities. The β-cyclodextrins form complexes with lipids and other hydrophobic molecules, and are therefore often used to destroy cholesterol-rich sub-domains of the plasma membrane [28]. Assuming that Taar1 retention in the compartments of the secretory pathway was caused by the destruction of primary cilia upon cathepsin activity inhibition in FRT cells, disruption of primary cilia via β-cyclodextrin should cause similar effects to those obtained with cathepsin inhibitor treatment. Indeed, Taar1 was retained in the compartments of the secretory

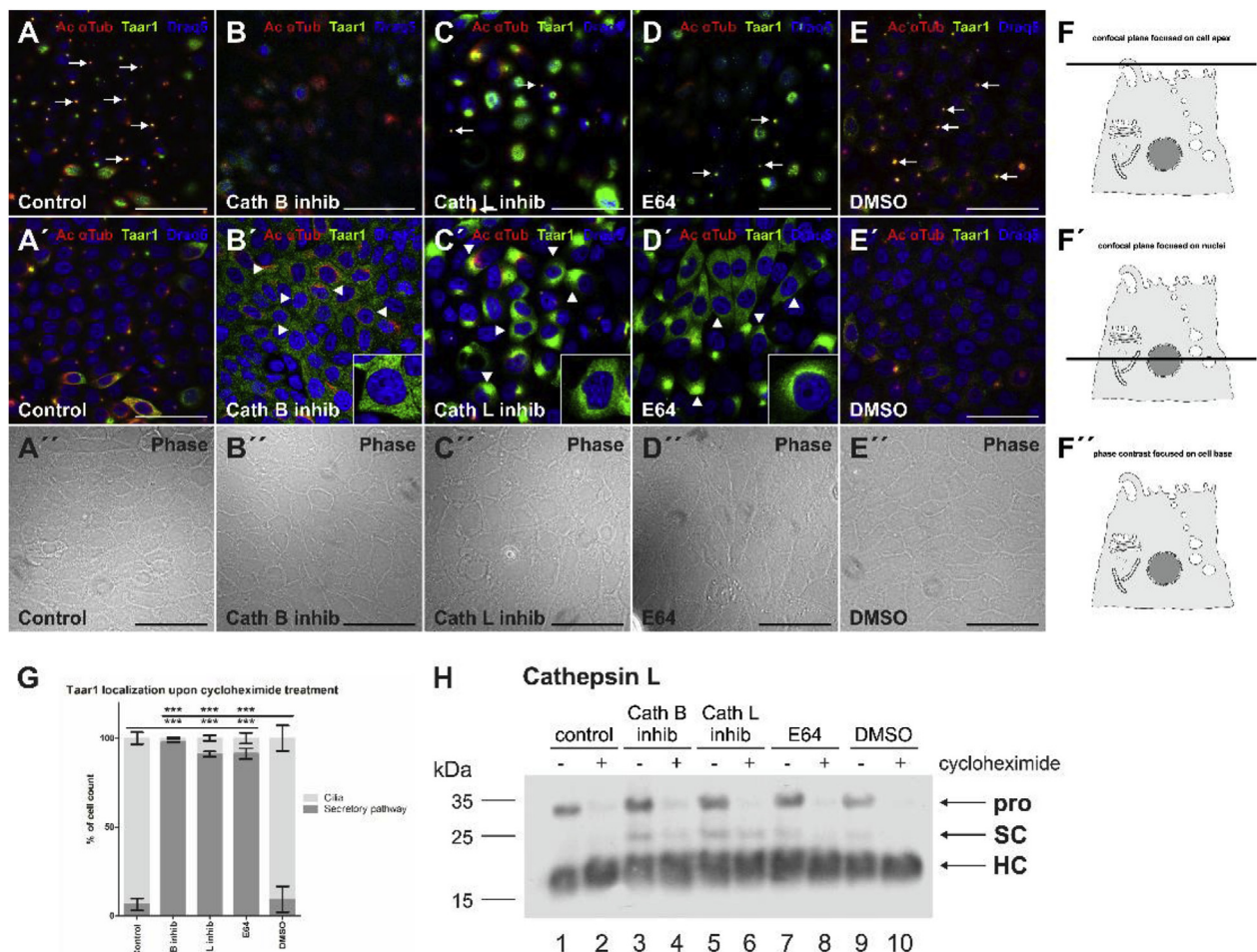


Fig. 6. Sub-cellular localization of Taar1 in FRT cells treated with cathepsin inhibitors and cycloheximide

FRT cells treated with cathepsin inhibitors as indicated and controls, all with addition of cycloheximide were stained with anti-Taar1 (green signals) and anti-acetylated α-tubulin (red signals) antibodies. Sketches in F and F' indicate where optical sections were positioned. Respective corresponding phase contrast images are depicted in A''-E''. The graph (G) represents the proportion of FRT cells characterized by sub-cellular localization of Taar1 confined to the compartments of secretory pathway (dark grey), or at primary cilia (light grey). As a control for successful inhibition of *de novo* protein biosynthesis, cathepsin L forms (as indicated) were immunoblotted in cell lysates upon incubation without (–) or with (+) cycloheximide (H).

Taar1 was localized mostly in the primary cilium in non- and DMSO-treated FRT cells (A and E, arrows), and in compartments of the secretory pathway in inhibitor-treated cells (B'-D', arrowheads). Localization in the rER is inferred from anti-Taar1-positive stainings of the nuclear envelope (B'-D', insets).

Scale bars represents 50 µm. A molecular mass marker is indicated in the left margin (G). Data are depicted as means ± standard deviations, ***P < 0.001. Numbers of cells analyzed via immunofluorescence: Control n = 550, Cath B inhib n = 601, Cath L inhib n = 463, E64 n = 414, DMSO n = 636.

pathway upon β -cyclodextrin treatment (Fig. 7, B' and E, arrowheads), while it was confined to primary cilia in non-treated cells (Fig. 7, A and D, arrows). The results reveal Taar1's presence in β -cyclodextrin-sensitive microdomains of the apical plasma membrane of FRT cells, which are identified as cilia due to the co-localization of Taar1 and acetylated α -tubulin (see Figs. 5 and 6 above), a notion supporting our previous report of Taar1 at primary cilia in this cell line [1].

3.7. Sub-cellular localization of Taar1 in FRTL-5 cells and absence of primary cilia

After we confirmed that Taar1 localization in FRT cells is dependent on cathepsin activity affecting the presence and maintenance of primary cilia, we aimed to determine Taar1 localization in less well-polarized, but functionally fully differentiated and

thyroglobulin-synthesizing thyrocytes *in vitro*. To this end, FRTL-5 cells were cultured until confluence before they were fixed and co-stained with rabbit anti-mouse Taar1 antibodies and polyclonal mouse anti-human Golgin97 or polyclonal mouse anti-human lysosome-associated membrane protein 2 (Lamp2) antibodies which were used as Golgi apparatus and lysosome markers, respectively. Lysosomes of FRTL-5 cells were also stained with the fluid phase marker LysoTracker Red DND-99, and plasma membrane constituents were stained with the lectin Concanavalin A.

In FRTL-5 cells, TAAR1 was found to be localized in the compartments of the secretory pathway (Fig. 8, A, arrowheads), namely in the endoplasmic reticulum (Fig. 8, B, arrowhead) and the Golgi apparatus (Fig. 8, C, arrowhead, yellow signals), and occasionally at the plasma membrane (Fig. 8, D and F, arrows, yellow signals). Taar1 was not observed in lysosomes of FRTL-5 cells (Fig. 8, E, arrowheads, red signals). Quantitation (data not shown) revealed

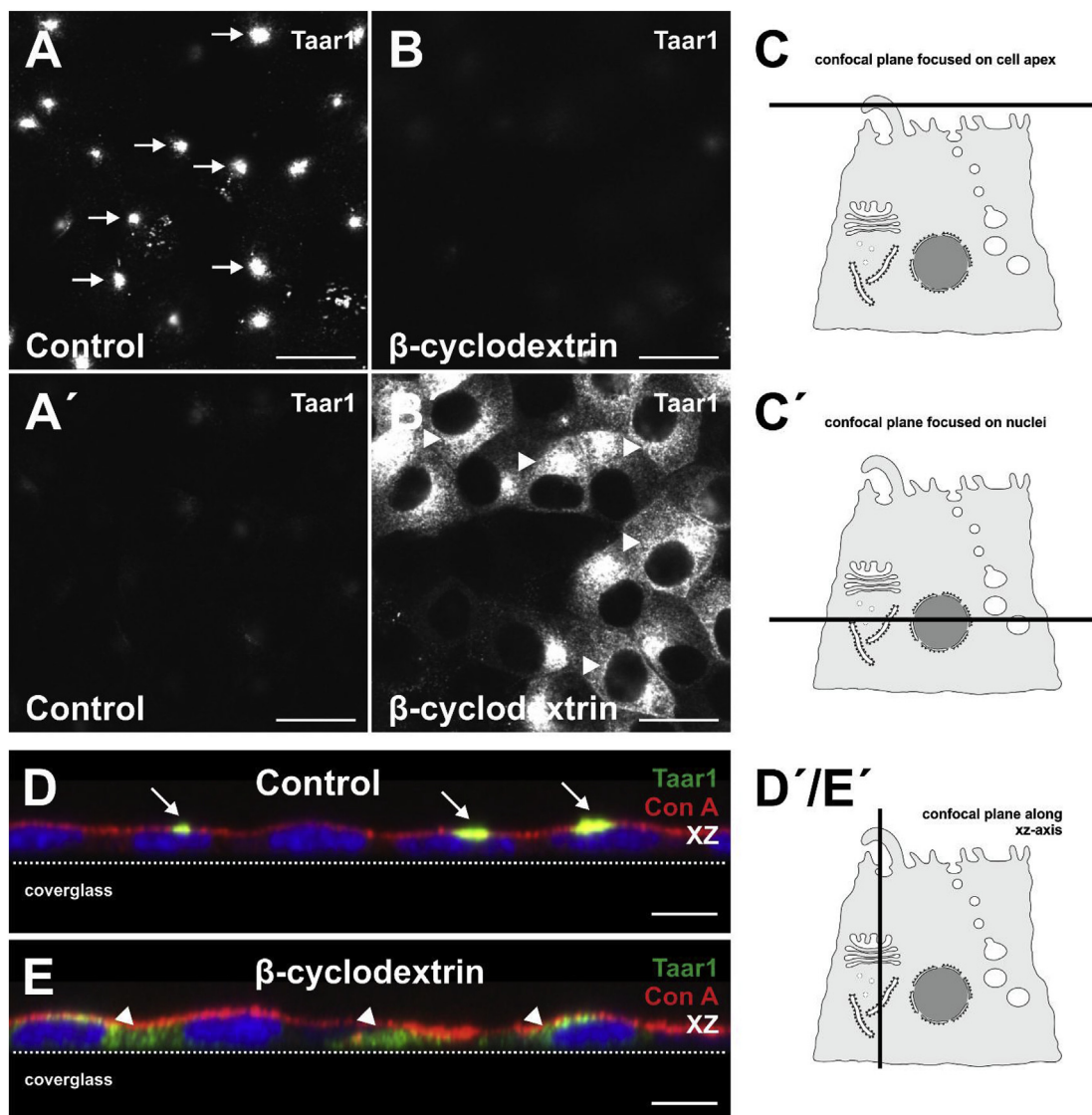


Fig. 7. Taar1 is retained in compartments of the secretory pathway in FRT cells treated with β -cyclodextrin

FRT cells treated with β -cyclodextrin were stained with anti-Taar1 antibodies (A-B', and green signals in D-E) and with Concanavalin A in order to highlight plasma membrane constituents (red signals in D-E). Sketches in C, C', and D'/E' indicate where optical sections were positioned. Images in D and E are xz-projections of z-stacks of images taken in the xy-mode, dotted lines represent the positions of the cover glasses.

Note that Taar1 was re-localized from primary cilia (arrows) to compartments of the secretory pathway (arrowheads) upon β -cyclodextrin treatment. Nuclei were counter-stained with Draq5™ (blue signals in D and E). Scale bars represent 50 μ m (A-B') and 5 μ m (D and E).

Taar1 to be localized in compartments of the secretory pathway in the majority of FRTL-5 cells (Fig. 8, A, arrowheads), while Taar1 localization at the plasma membrane was detected in only a minority of FRTL-5 cells (Fig. 8, A, arrows). FRTL-5 cells were stained with mouse anti-rat acetylated α tubulin antibodies in order to determine the principle presence of primary cilia in this cell line. It appeared that ciliogenesis occurs in FRTL-5 cells, but it is limited to a small number of cells within the population of cultured cells (Fig. 8, G and G', arrows).

3.8. Taar1 localization remains largely unaffected in FRTL-5 cells upon cathepsin activity inhibition

Next, we determined the effect of cathepsin activity inhibition on Taar1 localization in FRTL-5 cells, which were treated with cathepsin inhibitors as described for FRT cells and stained with rabbit anti-mouse Taar1 antibodies, while the glycoconjugates of the cell surface were counter-stained with concanavalin A.

Taar1 localization remained mainly unaltered in FRTL-5 cells upon treatment with cathepsin B or L inhibitors, and E64, in comparison to non-treated cells and vehicle control (Fig. 9A–E). Only a few cells in the non-treated FRTL-5 cells were characterized by Taar1 prevalence at extensions of the plasma membrane, thus resembling short primary cilia (Fig. 9, A, arrow), while in most cells Taar1 was localized in compartments of the secretory pathway (Fig. 9, A, arrowhead). Upon cathepsin inhibitor treatment, Taar1 was localized in compartments of the secretory pathway in most if not all FRTL-5 cells within a given cell culture (Fig. 9, B–D, arrowheads). However, similar results were observed in FRTL-5 cells treated with DMSO (Fig. 9, E, arrowheads). Thus, Taar1 distribution in FRTL-5 cells was not affected by cathepsin inhibitor treatment. Specificity of protease inhibitor treatment of FRTL-5 cells was proved by means of labelling with the broad spectrum ABP for all cysteine peptidases DCG-04 (Fig. 9, A'–E') and the cathepsin B-specific ABP NS-173 (Fig. 9, A'–E'').

3.9. Trafficking of Taar1 to the plasma membrane of rat thyrocytes is dependent on the presence of primary cilia

Taar1 co-localization with acetylated α tubulin in FRT and FRTL-5 cells revealed that Taar1 was localized in compartments of the secretory pathway only in cells that were lacking primary cilia (Fig. 10, A–B'', arrowheads). Consequently, in the presence of primary cilia, Taar1 was not retained in compartments of the secretory pathway (Fig. 10, A–B'', arrows). Instead, Taar1 was localized at the primary cilia of these cells. Thus, we reasoned that presence of primary cilia might be one of the factors determining the heterogeneity in distribution and sub-cellular localization of Taar1 among cell populations of rat thyrocytes *in vitro*. The data indicated the necessity of primary cilia present and maintained at the apical plasma membrane in order to enable Taar1 trafficking to these antenna-like projections of rat thyrocytes. If Taar1 were indeed acting as a sensor of the colloid state [1,7] (Fig. 11), the notion of Taar1's significance for TSH-regulated thyroid states [8] becomes all the more important, specifically, regarding co-regulation of cysteine cathepsin-mediated thyroglobulin processing by Taar1 at the apical cilia and the basolateral TSH receptors.

4. Discussion

Previously, the GPCR Taar1 was found at cilia of the apical plasma membrane domain of mouse thyrocytes *in situ* and rat thyrocytes *in vitro*, as demonstrated for FRT cells [1]. Primary cilia, typically up to a few micrometers in length and ca. 200 nm in diameter, are antennae-like projections abundant at the apical plasma membrane domain of most epithelial cells. Thyrocytes bear primary cilia which are shorter in length and broader in diameter in comparison to other epithelial cell types (this study and [1]). The microtubular axoneme of the primary cilium is anchored in the basal body, composed of acetylated α -tubulin, and surrounded by a membrane which is distinct in its composition from the remaining plasma membrane by virtue of a so-called transition zone (reviewed in [29]). Acetylated α -

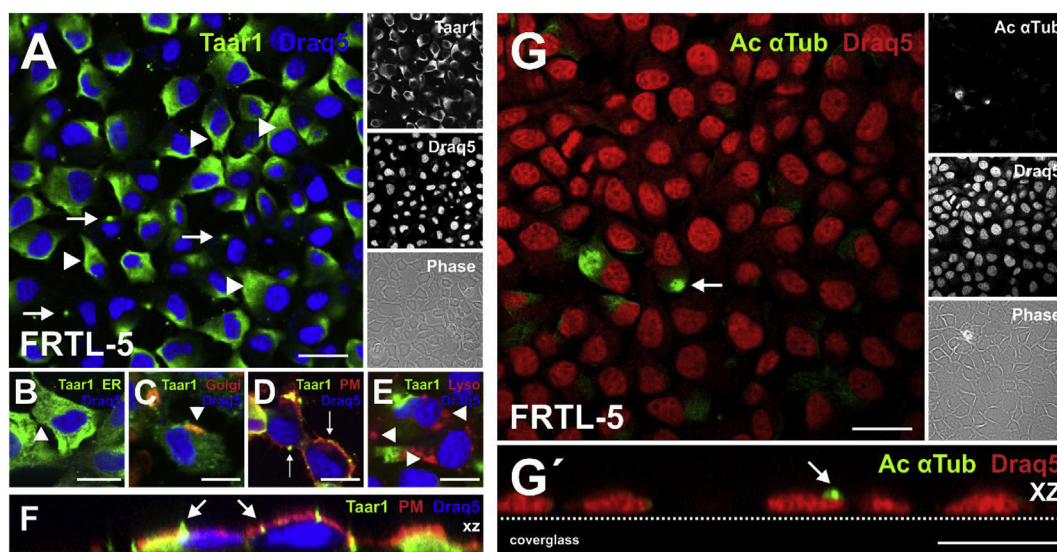


Fig. 8. Sub-cellular localization of Taar1 and presence of primary cilia in FRTL-5 cells

FRTL-5 cells were immunolabeled with anti-Taar1 antibodies (green signals, A–F). Cell compartments were labeled with specific markers (red signals, C–F): anti-Golgin97 antibody (Golgi apparatus, C), concanavalin A (plasma membrane, D), and LysoTracker Red DND-99 (lysosomes, E). Single channel fluorescence micrographs and corresponding phase contrast micrographs are depicted in right panels as indicated (A and G). Images in F and G' represent xz-projections of z-stacks of images taken in the xy-mode, dotted lines represent the positions of the cover glass.

Taar1 was localized at the apical plasma membrane domain (arrows) and in the compartments of secretory pathway (arrowheads), while it was not localized in lysosomes of FRTL-5 cells (E, arrowheads). Note that primary cilia were present in distinct FRTL-5 cells (G and G', arrows), only.

Nuclei were counter-stained with Draq5™ (blue signals A–F, red signals G and G'). Scale bars represent 10 μ m.

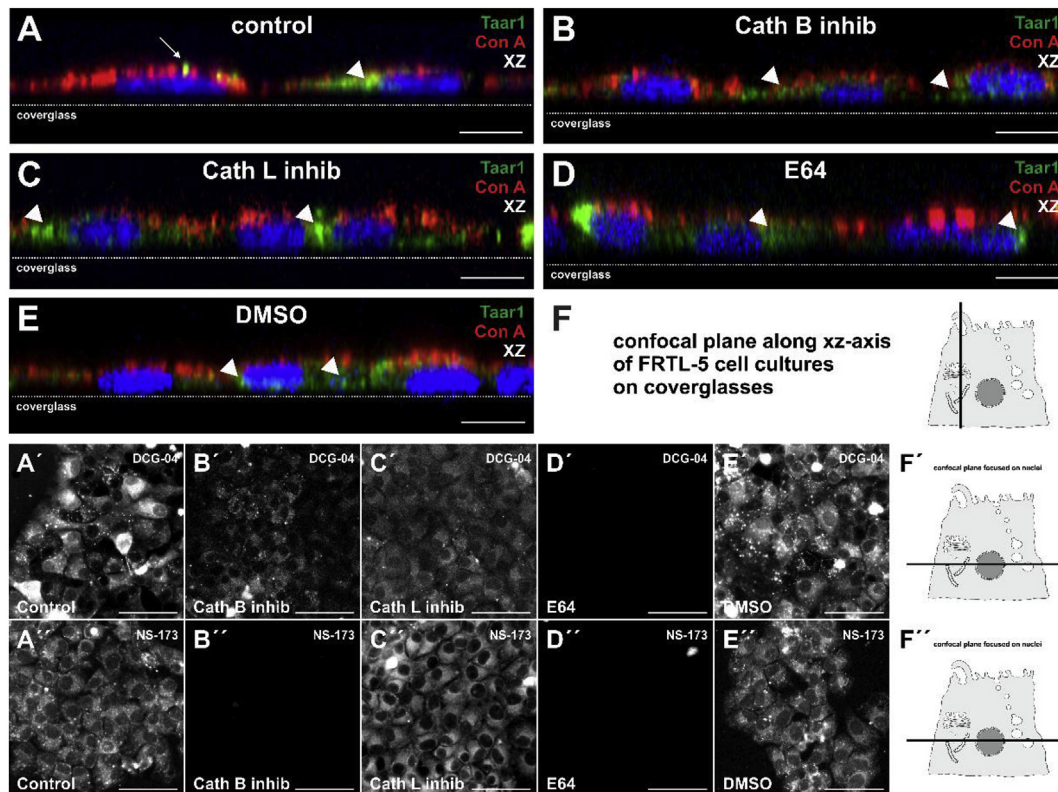


Fig. 9. Sub-cellular localization of Taar1 in FRTL-5 cells treated with cathepsin inhibitors and proof of inhibitor specificities

FRTL-5 cells treated with cathepsin inhibitors, and controls (as indicated) were stained with anti-Taar1 antibodies (A-E, green signals) and Concanavalin A (red signals). Images in A-E are xz-projections of z-stacks of images taken in the xy-mode as depicted by the sketch (F), dotted lines represent the positions of the cover glass. Note that the sub-cellular localization of Taar1 was mostly confined to the compartments of the secretory pathway of FRTL-5 cells (A-E, green signals, arrowheads) upon all treatment conditions. Taar1 was also found at the plasma membrane (A, arrow) in a small fraction of non-treated FRTL-5 cells (A, control). In control experiments, FRTL-5 cells were treated with cathepsin inhibitors as indicated, followed by incubation with DCG-04 Red (A'-E') or 10 μ M NS-173 Rhodamine (cathepsin B-specific activity based probe; A''-E'') and confocal imaging as sketched (F, F'), indicating specificities of protease inhibitors used. Nuclei were counter-stained with Draq5™ (A-E, blue signals). Scale bars represent 5 μ m (A-E) and 25 μ m (A'-E'').

tubulin was used in this and our previous study [1] as a cilia marker revealing co-localization with Taar1. Primary cilia are implicated in numerous receptor-mediated signalling pathways, e.g. Hedgehog and platelet-derived growth factor receptor A signalling [30–32]. Interestingly, trafficking of membrane proteins, accumulation of cytosolic secondary messengers, and positioning of effector proteins to primary cilia are restricted by the transition zone [33]. Therefore, the protein composition of the primary cilium is distinct from the plasma membrane protein contents and, likewise, calcium and cAMP concentrations are locally distinct in the cilia-associated cytosol [31,34–38]. A lack of the primary cilium or disturbances in its length and protein composition are known from ciliopathies, diseases that affect, among other organs, the brain and kidney [39–42]. Very recently, the absence of cilia from mouse thyroid epithelial cells has been connected to the development of signs of follicular and papillary thyroid cancer [43], indicating the importance of ciliogenesis for formation of cilia as indicators of the differentiated state of thyrocytes.

Thyroid epithelial cells are unique endocrine cells that secrete both, the thyroid hormone precursor thyroglobulin, and thyroglobulin processing proteases, the cathepsins, via their apical plasma membrane domain. Recently, Taar1-mediated signalling was shown by us to affect the protein amounts and activities of cathepsins B and L, as demonstrated in male Taar1-deficient mice [8]. Interestingly, we found cathepsin L at the primary cilia of porcine thyrocytes freshly isolated and kept in culture for few days [9], which could suggest, in principle, a possible interaction of this

protease with Taar1 at the apical pole of thyrocytes *in situ*. Because cathepsin L is essential for thyroglobulin processing and thyroid hormone liberation in rodents [4], we proposed that Taar1 at cilia acts as a sensor of the state of thyroglobulin processing in the thyroid follicle lumen ([1]; reviewed in [7]). Hence, here we designed a study to investigate interactions between proteolytic activity of cathepsins and sub-cellular localization of Taar1, in order to gain insights into possible interaction of cathepsin-mediated effects and Taar1-mediated signalling.

4.1. Taar1 is co-localized with cathepsin L at the primary cilia of FRT cells

In this study, we confirmed Taar1 expression in FRT cells via RT-PCR. In addition, we observed that cathepsin L is secreted from FRT cells and co-localized with Taar1 at the primary cilium. However, when we analyzed sub-cellular localization of cathepsin B in the same cell line, we found that cathepsin B is secreted in smaller amounts and is not localized at primary cilia to a similar extent. Previously, we have shown that cathepsin S was localized in vesicles distinct from vesicles containing related cathepsins in the human thyroid gland [44]. Hence, trafficking of cathepsins B and L in distinct and separate vesicles could be an underlying reason for the herein observed divergence in cathepsin B and L protein amounts secreted from FRT cells. Furthermore, the presence of binding sites specific for cathepsin L at the primary cilium of FRT cells could explain, in principle, the difference in sub-cellular

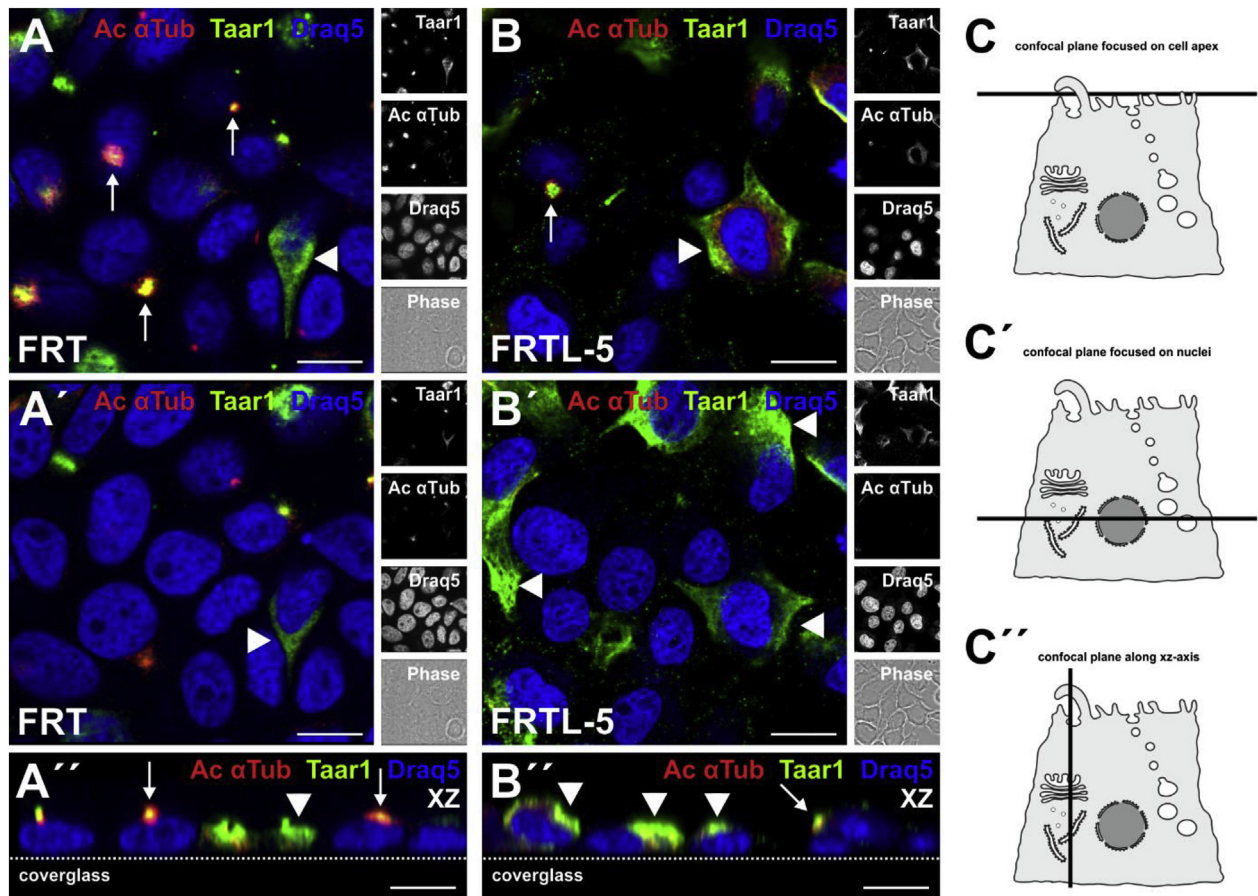


Fig. 10. Co-staining of Taar1 and acetylated α -tubulin in FRT and FRTL-5 cells

FRT and FRTL-5 cells were stained with anti-Taar1 (green signals) and anti-acetylated α -tubulin antibodies (A–B', red signals). Single confocal sections were taken at the top and median poles of FRT and FRTL-5 cells as indicated in the respective sketches (C–C'). Single channels, overlays of different channels, and corresponding phase contrast micrographs are depicted as indicated. Images in A'' and B'' are xz-projections of z-stacks of images taken in the xy-mode, dotted lines represent the positions of the cover glasses. Note that Taar1 is localized mostly at the primary cilium of FRT cells (A–A'', arrows), while it is less often found at primary cilia of FRTL-5 cells (B–B''). Taar1 is retained in compartments of the secretory pathway in particular in individual thyrocytes of either cell line when they lack primary cilia (A–B'', arrowheads). Nuclei were counter-stained with Draq5TM (blue signals). Scale bars represent 10 μ m.

localization between cathepsins B and L. However, the nature of cathepsin binding sites at the apical plasma membrane of thyrocytes adjacent to the thyroid follicle lumen is not yet fully understood, and investigations have so far only included the aspartic cathepsin D but less attention was paid to cysteine cathepsin binding to thyrocytes [7,17,45].

In other cellular systems, namely in colorectal carcinoma cells it was shown that secreted and proteolytically active cathepsin B re-associates with the plasma membrane in flask-like indentations, the caveoli [46,47]. Additionally, cathepsin B binding sites may include the LDL-receptor related proteins [48], the LRP, which are present at the apical plasma membrane but not necessarily localized to cilia. In general, cathepsins can re-associate with the plasma membrane also by binding to the cation-independent mannose 6-phosphate receptors, which serve in a safe-guarding system to recapture excessively secreted lysosomal enzymes, but are also not localized to cilia. Therefore, the molecular nature of cathepsin binding sites at the apical, lumen-apposed surface of thyroid epithelial cells remains elusive (see Ref. [7] for a recent review).

4.2. Sub-cellular localization of Taar1 is altered in FRT cells upon cathepsin inhibitor treatment

Several studies indicated importance of protease-mediated

actions on signal transduction, transmembrane protein trafficking, and receptor processing [49,50]. For instance, cathepsin B-mediated activity was found to prolong Toll-like receptor 2 (TLR2)/NF- κ B (nuclear factor kappa-light-chain-enhancer of activated B cells) activation in fibroblasts, and the serine protease inhibitor aprotinin was proposed to affect the recycling rates and density of epithelial Na⁺ channels at the plasma membrane in renal cells [50,51].

Here, we analyzed the effects of cathepsin activity on sub-cellular localization of Taar1, because this GPCR at the apical surface of thyroid epithelial cells co-regulates thyroid function in mice [8]. We determined the cross-talk between cathepsins and Taar1 in a well-established and highly polarized rodent thyroid cell line, the FRT cells, upon inhibition of the proteolytic activity of cathepsin L in comparison with cathepsin B inhibitor treatment. Previously, we showed that FRT cells are characterized by heterogeneity of sub-cellular distribution patterns of Taar1 among individual cells of the cell population [1]. Interestingly, here we show that inhibition of the proteolytic activity of cathepsin L caused differences in the pattern of sub-cellular localization of Taar1 among FRT cells. We observed that, in contrary to non-treated cells, Taar1 was confined to the secretory pathway in the majority of cathepsin L inhibitor-treated cells. Furthermore, similar effects were observed in cathepsin B inhibitor- and E64-treated cells, suggesting indirect effects of cathepsin activity inhibition on the subcellular

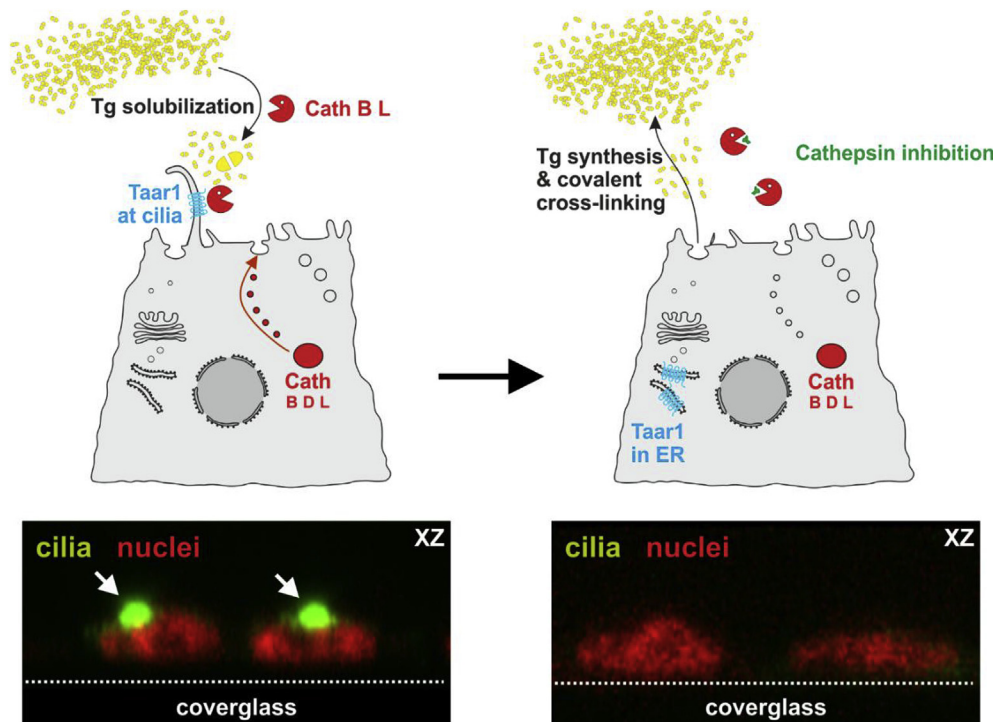


Fig. 11. Summarizing schematic sketch suggesting Taar1 at apical cilia as a co-regulator of cysteine cathepsin-mediated thyroglobulin processing for thyroid hormone liberation

Thyroglobulin (Tg), the thyroid hormone precursor molecule, is stored in the extracellular follicle lumen in covalently cross-linked form (left). Short-term TSH receptor signalling triggers secretion of endo-lysosomal enzymes at the apical pole (red arrow) for subsequent re-association with cilia in co-localization with Taar1. Luminal cysteine cathepsin-mediated thyroglobulin solubilization and processing yields release of thyroperins that potentially act as cysteine peptidase inhibitors. In analogy to the results of this study, we propose that such thyroperin-mediated cathepsin inhibition at the apical pole triggers disappearance of cilia and re-location of Taar1 to the endoplasmic reticulum (right). Hence, we propose that Taar1 at apical cilia (bottom left, arrows), which are present in resting follicles, acts as a sensor of thyroglobulin degradation states and co-regulates thyroid function that depends upon proteolytic action of cysteine cathepsins at extra-, peri- and intracellular locations.

localization of Taar1 in FRT cells, because cathepsin L did, but cathepsin B did not co-localize to the same extent with Taar1 in FRT cells. In addition, we confirmed that the observed alterations in sub-cellular localization of Taar1 upon cathepsin B and L inhibitor treatment are not due to *de novo* biosynthesis of Taar1 in the endoplasmic reticulum, because the effect was not changed upon cycloheximide treatment. Therefore, we conclude that trafficking of Taar1 depends on proper cathepsin activity levels.

Moreover, we asked whether Taar1 might be retained in the secretory pathway and might not reach the primary cilium due to disturbances in its morphology and structure. In order to test the validity of this hypothesis, we determined if the primary cilium is present in FRT cells upon inhibition of the proteolytic activity of cathepsins. Cathepsin B or L inhibitor- and E64-treated FRT cell populations were composed mainly of cells that lacked a primary cilium. In order to further confirm that Taar1 is retained in the secretory pathway in the absence of a primary cilium at the apical plasma membrane domain, we disrupted the structure of the primary cilium by β -cyclodextrin treatment of FRT cells. Indeed, disruption of the primary cilia of FRT cells caused Taar1 retention in the secretory pathway. However, the molecular pathway responsible for the disappearance of primary cilia upon cathepsin inhibitor treatment remains elusive.

In order to further confirm that the presence of primary cilia is essential for Taar1 trafficking to the plasma membrane, we investigated sub-cellular localization of Taar1 in non-polarized thyrocytes lacking a primary cilium. We selected an appropriate less well-polarized rat cell lines, namely FRTL-5 cells. When confirming the expression of Taar1 in this cell line, we observed that FRTL-

5 cells, like the FRT cells, from which they are derived, were characterized by little heterogeneity of Taar1 distribution among the cell population. Hence, the percentages of Taar1 prevalence in the secretory pathway and at the plasma membrane in FRTL-5 cells were highly dissimilar to FRT cells. A vast majority of FRTL-5 cells expressed Taar1 in the secretory pathway, while only a few cells in the cell population expressed Taar1 at the plasma membrane. In addition, Taar1 was localized at the plasma membrane of only those FRTL-5 cells that possessed primary cilia. It is noteworthy, that, similarly, non-treated FRT cells characterized by Taar1 presence in the secretory pathway also lacked a primary cilium.

We conclude that a primary cilium is essential for Taar1 to be trafficked to the plasma membrane of rat thyrocytes *in vitro*. The fact that sub-cellular localization of Taar1 was not drastically altered upon cathepsin inhibition in the less well-polarized FRTL-5 cells leads to the conclusion that the downstream action of cysteine protease inhibitors compromises the stability of the primary cilium, but does not directly affect Taar1 trafficking.

Therefore, future studies will need to involve investigations on the molecular regulation of both, ciliogenesis and Taar1 transport to cilia as well as its potential diffusion for precise positioning when arrived at these cellular extensions of thyrocytes. Molecules known to affect the ultrastructure of cilia as well as the motion of proteins to and along them [52,53], such as intraflagellar transport 88 (Ift88) and Ift20, are expressed in mouse thyroid epithelial cells (our own unpublished observations). However, in a mouse model among others deficient in the cysteine cathepsin K that is redundantly expressed with and functionally compensated by cathepsin L in thyroid tissue, transcript levels of Ift proteins are not altered in

comparison to wild type (our own unpublished observations). Thus, we propose molecular mechanisms other than regulated by Ift proteins involve in Taar1 transport to and along cilia of rodent thyroid epithelial cells.

5. Conclusions

This study has elucidated that Taar1 trafficking in the rodent thyroid is subject to the polarity and differentiation states of thyroid epithelial cells, and depends on the presence and activity of proteases like the cysteine cathepsins, which maintain the cilia of thyroid epithelial cells intact and extended. Hence, the results of this study are well in line with our previous investigations regarding the presence of cilia in cultures of primary porcine thyrocytes [9]. In addition, cilia were also detected in thyroid epithelial cells of mice [1,43] and rats [1] as well as in human thyroid tissue [54], indicating that primary cilia at the thyroid follicle lumen-apposed apical plasma membrane are a common feature of mammalian thyroid epithelial cells.

Moreover, in a very recent study by the group of Inés Martín-Lacave, normal human thyroid tissue was analyzed by means of fluorescence microscopy of immunolabeled sections, and by transmission or scanning electron microscopy, to determine the presence of primary cilia with an average length of about $3.93 \pm 0.9 \mu\text{m}$ [54]. Interestingly and similar to our previous [1] and this study, the authors found a frequency of one cilium per cell, while only approx. 75% of all cells in normal thyroid tissue were ciliated. In addition, cilia shortening and/or disappearance was observed predominantly in hyperactive follicles in human thyroid tissue taken from pathological states such as nodular hyperplasia or Graves' disease [54]. In analogy, TSH-stimulated activity of thyroid epithelial cells is characterized by thyroglobulin degradation mediated by the secreted cysteine cathepsins B, K, L or S [4,9,44], which we proposed yields unmasking of internal thyropin sequences [5,7]. Thyropins are cysteine peptidase inhibitors derived from thyroglobulin itself [55, 56], which could act in a manner simulated in this study, namely, from the cells' apexes.

Consequently, the relocation of Taar1 to the rER upon inhibition of cathepsins, such as observed herein for FRT cells, may serve a vital physiological function, namely the sensing of thyroglobulin processing in the lumina of thyroid follicles for maintenance of follicular homeostasis (see Fig. 11). In our suggested model, resting thyroid follicles feature well-polarized thyrocytes which bear a primary cilium hosting Taar1 that reaches out into the follicle lumen filled with non-processed thyroglobulin storage forms. Upon TSH receptor signalling, and hence, thyroid follicle activation, endolysosomal cathepsins are recruited and trafficked to the apical plasma membrane for subsequent secretion into the follicle lumen and thyroglobulin processing, which yields among solubilized thyroglobulin and some thyroxine also the thyropins. By way of inhibition and thus termination of cathepsin-mediated thyroglobulin processing, also the presence of Taar1 at cilia and the extension of cilia themselves will be temporarily altered, namely such that Taar1 is relocated to the rER and the cilia will shorten or even disappear altogether. This may coincide with TSH receptor internalization [8] resulting in altered signalling, thus initiating thyroglobulin re-synthesis at the rER. Subsequently, trafficking along the secretory pathway is triggered to transport thyroglobulin to the apical plasma membrane domain for iodination upon secretion and before storage. During this phase of luminal re-filling with thyroglobulin, also Taar1 can be trafficked to the cell surface, since cilia reform and extend, thereby starting another round of the thyroglobulin storage phase of resting follicles. In fact, we suggest that the extent of thyroglobulin storage in osmotically inert, covalently cross-linked form in the thyroid follicle lumen can be sensed by

(re-)extended cilia hosting Taar1 that acts – together with TSH receptors – as a co-regulator of thyroid homeostasis [7,8]. By this scenario, the direct relationship between ciliogenesis and follicle activity, as proposed by us [1,7,8] and others [54], could be explained mechanistically at the cellular and molecular levels. In summary, cysteine cathepsins and cross-talk between Taar1 and the TSH receptors are important for regular thyroid physiology.

This proposal requires further experimentation but provides an important cellular mechanism that would also explain the heterogeneity of thyroid follicle states within the thyroid gland inspected at any given time (for review, see [7]).

Funding

This work was supported by the Deutsche Forschungsgemeinschaft (Bonn, Germany) in the framework of SPP 1629 Thyroid Trans Act [BR1308/11–1 and 11–2].

Author contributions

JS and KB devised the study; JS, ZB, AAH, VV and VS conducted the experiments; MB and NS designed, synthesized and validated activity based probes and specific cysteine cathepsin inhibitors; all authors contributed to data interpretation and manuscript writing; all authors have approved the final version of the manuscript.

Declarations of interest

None.

References

- [1] J. Szumska, et al., Trace amine-associated receptor 1 localization at the apical plasma membrane domain of Fisher rat thyroid epithelial cells is confined to cilia, *Eur. Thyroid J.* 4 (2015) 30–41, <https://doi.org/10.1159/000434717>.
- [2] J. Lerman, Iodine components of the blood. circulating thyroglobulin in normal persons and in persons with thyroid disease, *J. Clin. Investig.* 19 (1940) 555–560, <https://doi.org/10.1172/jci101158>.
- [3] W. Tong, A. Taurig, I.L. Chaikoff, Non-thyroglobulin iodine of the thyroid gland. I. Free thyroxine and diiodotyrosine, *J. Biol. Chem.* 191 (1951) 665–675.
- [4] B. Friedrichs, et al., Thyroid functions of mouse cathepsins B, K, and L, *J. Clin. Investig.* 111 (2003) 1733–1745, <https://doi.org/10.1172/jci15990>.
- [5] K. Brix, M. Linke, C. Tepel, V. Herzog, Cysteine proteinases mediate extracellular prohormone processing in the thyroid, *Biol. Chem.* 382 (2001) 717–725, <https://doi.org/10.1515/bc.2001.087>.
- [6] S. Dauth, M. Arampatzidou, M. Rehders, D.M.T. Yu, D. Fuhrer, K. Brix, Thyroid cathepsin K – roles in physiology and thyroid disease, *Clin. Rev. Bone Miner. Metabol.* 9 (2011) 94–106, <https://doi.org/10.1007/s12018-011-9093-7>.
- [7] K. Brix, M. Qatato, J. Szumska, V. Venugopalan, M. Rehders, Thyroglobulin storage, processing and degradation for thyroid hormone liberation, in: M. Luster, L. Duntas, L. Wartofsky (Eds.), *The Thyroid and its Diseases*, Springer International Publishing AG, part of Springer Nature, 2019, https://doi.org/10.1007/978-3-319-72102-6_3.
- [8] M. Qatato, J. Szumska, V. Skripnik, E. Rijntjes, J. Kohrle, K. Brix, Canonical TSH regulation of cathepsin-mediated thyroglobulin processing in the thyroid gland of male mice requires Taar1 expression, *Front. Pharmacol.* 9 (2018) 221, <https://doi.org/10.3389/fphar.2018.00221>.
- [9] K. Brix, P. Lemansky, V. Herzog, Evidence for extracellularly acting cathepsins mediating thyroid hormone liberation in thyroid epithelial cells, *Endocrinology* 137 (1996) 1963–1974, <https://doi.org/10.1210/endo.137.5.8612537>.
- [10] M.T. Nieman, Protease-activated receptors in hemostasis, *Blood* 128 (2016) 169–177, <https://doi.org/10.1182/blood-2015-11-636472>.
- [11] F.S. Ambesi-Impimbato, L.A. Parks, H.G. Coon, Culture of hormone-dependent functional epithelial cells from rat thyroids, *Proc. Natl. Acad. Sci. U. S. A.* 77 (1980) 3455–3459.
- [12] L. Nitsch, D. Tramontano, F.S. Ambesi-Impimbato, N. Quarto, S. Bonatti, Morphological and functional polarity of an epithelial thyroid cell line, *Eur. J. Cell Biol.* 38 (1985) 57–66.
- [13] H. Ishikawa, W.F. Marshall, Ciliogenesis: building the cell's antenna, *Nat. Rev. Mol. Cell Biol.* 12 (2011) 222–234, <https://doi.org/10.1038/nrm3085>.
- [14] D. Greenbaum, K.F. Medzihradsky, A. Burlingame, M. Bogoy, Epoxide electrophiles as activity-dependent cysteine protease profiling and discovery tools, *Chem. Biol.* 7 (2000) 569–581.
- [15] N. Schaschke, I. Assfalg-Machleidt, T. Lassleben, C.P. Sommerhoff, L. Moroder, W. Machleidt, Epoxysuccinyl peptide-derived affinity labels for cathepsin B,

- FEBS Lett. 482 (2000) 91–96.
- [16] K. Brix, S. Jordans, Watching proteases in action, *Nat. Chem. Biol.* 1 (2005) 186–187, <https://doi.org/10.1038/nchembio0905-186>.
 - [17] K. Brix, A. Dunkhorst, K. Mayer, S. Jordans, Cysteine cathepsins: cellular roadmap to different functions, *Biochimie* 90 (2008) 194–207, <https://doi.org/10.1016/j.biochi.2007.07.024>.
 - [18] G. Chiellini, et al., Cardiac effects of 3-iodothyronamine: a new aminergic system modulating cardiac function, *FASEB J.* 21 (2007) 1597–1608, <https://doi.org/10.1096/fj.06-7474com>.
 - [19] M.R. Lamprecht, D.M. Sabatini, A.E. Carpenter, CellProfiler: free, versatile software for automated biological image analysis, *Biotechniques* 42 (2007) 71–75, <https://doi.org/10.2144/000112257>.
 - [20] V. Neuhoﬀ, K. Philipp, H.G. Zimmer, S. Mesecke, A simple, versatile, sensitive and volume-independent method for quantitative protein determination which is independent of other external influences, *Hoppe Seylers Z. Physiol. Chem.* 360 (1979) 1657–1670.
 - [21] A.J. Barrett, Fluorimetric assays for cathepsin B and cathepsin H with methyloctamylamide substrates, *Biochem. J.* 187 (1980) 909–912.
 - [22] K. Mayer, A. Vreemann, H. Qu, K. Brix, Release of endo-lysosomal cathepsins B, D, and L from IEC6 cells in a cell culture model mimicking intestinal manipulation, *Biol. Chem.* 390 (2009) 471–480, <https://doi.org/10.1515/bc.2009.047>.
 - [23] D.A. Nelson, M.D. Tolbert, S.J. Singh, K.L. Bost, Expression of neuronal trace amine-associated receptor (Taar) mRNAs in leukocytes, *J. Neuroimmunol.* 192 (2007) 21–30, <https://doi.org/10.1016/j.jneuroim.2007.08.006>.
 - [24] M. Linke, V. Herzog, K. Brix, Trafficking of lysosomal cathepsin B-green fluorescent protein to the surface of thyroid epithelial cells involves the endosomal/lysosomal compartment, *J. Cell Sci.* 115 (2002a) 4877–4889.
 - [25] M. Linke, S. Jordans, L. Mach, V. Herzog, K. Brix, Thyroid stimulating hormone upregulates secretion of cathepsin B from thyroid epithelial cells, *Biol. Chem.* 383 (2002b) 773–784, <https://doi.org/10.1515/bc.2002.081>.
 - [26] H. Buth, et al., Cathepsin B is essential for regeneration of scratch-wounded normal human epidermal keratinocytes, *Eur. J. Cell Biol.* 86 (2007) 747–761, <https://doi.org/10.1016/j.ejcb.2007.03.009>.
 - [27] T. Tamhane, R. Llukumbura, S. Lu, G.M. Maelandsmo, M.H. Haugen, K. Brix, Nuclear cathepsin L activity is required for cell cycle progression of colorectal carcinoma cells, *Biochimie* 122 (2016) 208–218, <https://doi.org/10.1016/j.biochi.2015.09.003>.
 - [28] R. Zidovetzki, I. Levitan, Use of cyclodextrins to manipulate plasma membrane cholesterol content: evidence, misconceptions and control strategies, *Biochim. Biophys. Acta* 1768 (2007) 1311–1324, <https://doi.org/10.1016/j.bbamem.2007.03.026>.
 - [29] J.L. Rosenbaum, G.B. Witman, Intraflagellar transport, *Nat. Rev. Mol. Cell Biol.* 3 (2002) 813–825, <https://doi.org/10.1038/nrm952>.
 - [30] C. Dore, W. Alpaugh, L. Su, J. Biernaskie, I. Dobrinski, Primary cilia on porcine testicular somatic cells and their role in hedgehog signaling and tubular morphogenesis in vitro, *Cell Tissue Res.* 368 (2017) 215–223, <https://doi.org/10.1007/s00441-016-2523-6>.
 - [31] B.S. Moore, et al., Cilia have high cAMP levels that are inhibited by Sonic Hedgehog-regulated calcium dynamics, *Proc. Natl. Acad. Sci. U. S. A.* 113 (2016) 13069–13074, <https://doi.org/10.1073/pnas.1602393113>.
 - [32] F. Bangs, K.V. Anderson, Primary cilia and mammalian hedgehog signaling, *Cold Spring Harb. Perspect. Biol.* 9 (2017), <https://doi.org/10.1101/cshperspect.a028175>.
 - [33] S.S. Francis, J. Sfakianos, B. Lo, I. Mellman, A hierarchy of signals regulates entry of membrane proteins into the ciliary membrane domain in epithelial cells, *J. Cell Biol.* 193 (2011) 219–233, <https://doi.org/10.1083/jcb.201009001>.
 - [34] S.L. Bielas, et al., Mutations in INPP5E, encoding inositol polyphosphate-5-phosphatase E, link phosphatidylinositol signaling to the ciliopathies, *Nat. Genet.* 41 (2009) 1032–1036, <https://doi.org/10.1038/ng.423>.
 - [35] K.C. Corbit, P. Aanstad, V. Singla, A.R. Norman, D.Y. Stainier, J.F. Reiter, Vertebrate Smoothed functions at the primary cilium, *Nature* 437 (2005) 1018–1021, <https://doi.org/10.1038/nature04117>.
 - [36] M. Jacoby, et al., INPP5E mutations cause primary cilium signaling defects, ciliary instability and ciliopathies in human and mouse, *Nat. Genet.* 41 (2009) 1027–1031, <https://doi.org/10.1038/ng.427>.
 - [37] L. Milenkovic, M.P. Scott, R. Rohatgi, Lateral transport of Smoothed from the plasma membrane to the membrane of the cilium, *J. Cell Biol.* 187 (2009) 365–374, <https://doi.org/10.1083/jcb.200907126>.
 - [38] S. Mukhopadhyay, H.B. Badgandi, S.H. Hwang, B. Somatilaka, I.S. Shimada, K. Pal, Trafficking to the primary cilium membrane, *Mol. Biol. Cell* 28 (2017) 233–239, <https://doi.org/10.1091/mbc.E16-07-0505>.
 - [39] V. Cantagrel, et al., Mutations in the cilia gene ARL13B lead to the classical form of Joubert syndrome, *Am. J. Hum. Genet.* 83 (2008) 170–179, <https://doi.org/10.1016/j.ajhg.2008.06.023>.
 - [40] T. Caspar, C.E. Larkins, K.V. Anderson, The graded response to Sonic Hedgehog depends on cilia architecture, *Dev. Cell* 12 (2007) 767–778, <https://doi.org/10.1016/j.devcel.2007.03.004>.
 - [41] C. Hanke-Gogokhia, Z. Wu, C.D. Gerstner, J.M. Frederick, H. Zhang, W. Baehr, Arf-like protein 3 (ARL3) regulates protein trafficking and ciliogenesis in mouse photoreceptors, *J. Biol. Chem.* 291 (2016) 7142–7155, <https://doi.org/10.1074/jbc.M115.710954>.
 - [42] F. Hildebrandt, T. Benzing, N. Katsanis, Ciliopathies, *N. Engl. J. Med.* 364 (2011) 1533–1543, <https://doi.org/10.1056/NEJMr1010172>.
 - [43] J. Lee, et al., Loss of primary cilia results in the development of cancer in the murine thyroid gland, *Mol. Cells* (2019), <https://doi.org/10.14348/molcells.2018.0430>.
 - [44] S. Jordans, et al., Monitoring compartment-specific substrate cleavage by cathepsins B, K, L, and S at physiological pH and redox conditions, *BMC Biochem.* 10 (2009) 23, <https://doi.org/10.1186/1471-2091-10-23>.
 - [45] P. Lemansky, K. Brix, V. Herzog, Iodination of mature cathepsin D in thyrocytes as an indicator for its transport to the cell surface, *Eur. J. Cell Biol.* 76 (1998) 53–62, [https://doi.org/10.1016/S0171-9335\(98\)80017-4](https://doi.org/10.1016/S0171-9335(98)80017-4).
 - [46] D. Cavallo-Medved, J. Mai, J. Doseescu, M. Sameni, B.F. Sloane, Caveolin-1 mediates the expression and localization of cathepsin B, pro-urokinase plasminogen activator and their cell-surface receptors in human colorectal carcinoma cells, *J. Cell Sci.* 118 (2005) 1493–1503, <https://doi.org/10.1242/jcs.02278>.
 - [47] D. Cavallo-Medved, D. Rudy, G. Blum, M. Bogyo, D. Gaglio, B.F. Sloane, Live-cell imaging demonstrates extracellular matrix degradation in association with active cathepsin B in caveolae of endothelial cells during tube formation, *Exp. Cell Res.* 315 (2009) 1234–1246, <https://doi.org/10.1016/j.yexcr.2009.01.021>.
 - [48] C. Arkona, B. Wiederanders, Expression, subcellular distribution and plasma membrane binding of cathepsin B and gelatinases in bone metastatic tissue, *Biol. Chem.* 377 (1996) 695–702.
 - [49] R. Chen, G. Jin, T.M. McIntyre, The soluble protease ADAMDEC1 released from activated platelets hydrolyzes platelet membrane pro-epidermal growth factor (EGF) to active high-molecular-weight EGF, *J. Biol. Chem.* 292 (2017) 10112–10122, <https://doi.org/10.1074/jbc.M116.771642>.
 - [50] K. Sasamoto, et al., Analysis of aprotinin, a protease inhibitor, action on the trafficking of epithelial Na⁺ channels (ENaC) in renal epithelial cells using a mathematical model, *Cell. Physiol. Biochem.* 41 (2017) 1865–1880, <https://doi.org/10.1159/000471934>.
 - [51] X. Li, et al., Cathepsin B regulates collagen expression by fibroblasts via prolonging TLR2/NF- κ B activation, *Oxid. Med. Cell. Longev.* 2016 (2016) 7894247, <https://doi.org/10.1155/2016/7894247>.
 - [52] F. Oswald, B. Prevost, S. Acar, E.J.C. Peterman, Interplay between ciliary ultrastructure and IFT-train dynamics revealed by single-molecule super-resolution imaging, *Cell Rep.* 25 (2018) 224–235, <https://doi.org/10.1016/j.celrep.2018.09.019>.
 - [53] L.E. Weiss, L. Milenkovic, J. Yoon, T. Stearns, W.E. Moerner, Motional dynamics of single Patched1 molecules in cilia are controlled by Hedgehog and cholesterol, *Proc. Natl. Acad. Sci. U. S. A.* 116 (2019) 5550–5557, <https://doi.org/10.1073/pnas.1816747116>.
 - [54] J.M. Fernández-Santos, J.C. Utrilla, V. Vázquez-Román, J.L. Villar-Rodríguez, L. Gutiérrez-Avilés, I. Martín-Lacave, Primary cilium in the human thyrocytes: changes in frequency and length in relation to the functional pathology of the thyroid gland, *Thyroid* 29 (2019) 595–606, <https://doi.org/10.1089/thy.2018.0401>.
 - [55] Lenarcic B, Bevec T, Thyropins—new structurally related proteinase inhibitors, *Biol. Chem.* 379 (1998) 105–111.
 - [56] M. Mihelcic, D. Turk, Two decades of thyroglobulin type-1 domain research, *Biol. Chem.* 388 (2007) 1123–1130, <https://doi.org/10.1515/bc.2007.155>.